Studies on Viral Genes related to the Virulence of Equine Herpesvirus 9 and the Phylogenetics of Equine Herpesvirus

（ウマヘルペスウイルス 9 型の毒力関連遺伝子およびウマヘルペスウイルスの系統学に関する研究）

2014

The United Graduate School of Veterinary Sciences, Gifu University

(Gifu University)

GUO　Xiaoqin

CONTENTS

ABBREVIATIONS

bp	base pair
BS	Bit score
BSA	Bovine serum albumin
BSR	The homology bit score ratio
cDNA	complementaly Deoxyribonucleic Acid
CPE	cytopathic effect
Ct	Cycle threshold
DTT	Dithiothreitol
EHV-1	Equine herpesvirus type 1
EHV-4	Equine herpesvirus type 4
EHV-8	Equine herpesvirus type 8
EHV-9	Equine herpesvirus type 9
FBS	Fetal Bovine Serum
FEK	Fetal Equine kidney
FHK 3.1	Fetal Horse kidney 3.1
GFP	Green Fluorescent Protein
GST	Glutathione S-transferase
IPTG	Isopropyl β-D-1-thiogalactopyranoside
MDBK	Madin-Darby bovine kidney
MEM	Minimum Essential Medium
MOI	Multiplicity of infection
ORF	Open Reading Frame
PCR	Polymerase Chain Reaction
PBS	Phosphate buffered saline
pfu	Plaque Forming Unit
p.i	Post infection
qRT-PCR	Quantitative real-time Polymerase Chain Reaction
RK-13	Rabbit Kidney 13

RT-PCR	Reverse Transcription-Polymerase Chain Reaction
SDS-PAGE	Sodium dodecyl sulfate polyacrylamide gel electrophoresis
SPF	Specific Pathogen Free
SP21	Mutant strain of Equine Herpesvirus 9
T-529	Equine herpesvirus isolated from onager
T-616	Equine herpesvirus isolated from zebra
VHS	virion host shutoff
94-137	Equine herpesvirus isolated from gazelle

GENERAL INTRODUCTION

Equine herpesvirus type 9 (EHV-9) was isolated from a Thomson's gazelle suffering neurological disease, initially it was called gazelle herpesvirus 1 (GHV-1) (16). EHV-9 showed serological cross-reactivity with equine herpesvirus type 1 (EHV-1), and has a homology of approximately 95% to EHV-1 and EHV-8 (16, 17, 31). EHV-9 has neurotropism in a wide host range, is most closely related to neurotropic EHV-1 (15, 17). EHV-9 has been isolated from non-equine species like gazelle, giraffe, polar bears with neurologic symptoms in zoos (11, 16, 22, 27).

Equine herpesviruses consist of nine types from 1 to 9. Equine herpesvirus types 1, 3, 4, 6, 8 and 9 are classified into subfamily Alphaherpesvirinae genus Varicellovirus. Equine herpesvirus types 2, 5 and 7 belong to subfamily Gammaherpesvirnae genus Percavirus.

The complete genome sequence of EHV-9 (accession no. AP010838 in Genbank) consists of 148,371 bps in length and has 75 genes and 80 open reading frames (ORFs) found in EHV-1 strain Ab4p (accession no. AY665713 in Genbank)(17). 62 genes are in the unique long (UL) region, duplicated 4 genes are in each of the internal repeat (IR) region and terminal repeat (TR) regions, and 9 genes in the unique short (US) region. ORFs 42, 52 and 53 showed the highest identity to those in EHV-1 (95%), while ORF71 showed the lowest degree of identity (86%). Except that ORF68 has a frameshift, the others only have in-frame additions and deletions of codons (17). The experimental infection of EHV-9 indicated that EHV-9 causes latent nonsuppurative encephalitis in horses, cattle and pigs and fatal nonsuppurative encephalitis

followed by severe neurologic manifestation in goats, mice, rats, hamsters, guineapigs, dogs, cats, marmosets, giraffe and polar bear (11, 15, 27, 31, 38, 53, 54, 65, 66). Histopathological study in the experimental animals suggested that EHV-9 entered the brain through the olfactory nerve pathway and then spread in the brain (12). It was indicated that a hamster model can be used to evaluate neuropathogenicity of EHV-9 (15).

Analysis of both virus and host factors in virus pathotenicity is necessary to control virus infection. Genetic mutants might be an useful tool to reveal pathogenesis in an animal model. In general, mutation is known to easily occur in cultured cells derived from non-natural host, than in the cells derived from the natural host. Isolation of EHV-1 mutants has been examined using various cells such as Madin-Darby bovine kidney (MDBK), rabbit kidney (RK13), and baby hamster kidney (BHK-21) cells (3, 23, 50). It was reported for EHV-1 that mutant viruses between 8 and 11 passages in BHK-21 cells had a 0.8 kb deletion in the unique short region of the genome (49). The mutant virus was characterized on virological properties by using culture cells and animal models. The mutation region was confirmed by using restriction digestion and genome sequencing. On EHV-1, it was suggested that glycoprotein I (gI, ORF73), glycoprotein E (gE, ORF74), infected cell protein 4 (ICP4, ORF64) and DNA polymerase (ORF30) genes were related to neuropathogenicity (32, 39). However, homologues of these genes and their products in EHV-9 have never been analysed yet. The mechanism of neuropathogenicity of EHV-9 is still unclear.

Herpesviruses have been isolated from various animals. Some kind of herpesviruses may cross the species barrier to spread beyond their normal host

range (16). Zoos are the artificial place keeping a high diversity of animal species from different areas. It might provide the opportunities to spread pathogens to a unexpected host. A polar bear named Jerka(20-year-old, female), kept in a zoo in Berlin died of acute encephalitis, which was caused by the zebra-borne EHV-1 (22). Greenwood *et al.* indicated that the virus was a recombinant between EHV-1 and EHV-9 based on the nucleotide sequences of ORF30 encoding the virus DNA polymerase. EHV-1 is a major pathogen of horses all over the worlds, and associated with epidemics of abortion, respiratory tract disease and disorders of the central nervous system (55, 56). EHV-1 has been isolated from a number of equid species (36, 64) and non-equid species (29, 41). In recent years, fatal encephalitis induced by zebra-borne EHV-1 species transmission has been reported frequently (1, 22). Three virus isolated from zoo animals, zebra (T-616), onager (T-529), and gazelle (94-137), were related to horse-derived EHV-1s (18). Due to the polar bear Jerka's case, the possibility of recombination of EHV-1 and EHV-9 might be speculated for in these three viruses. The analysis of genome sequences of these three viruses becomes important. Recently, application of next generation DNA sequencers makes reading the 150 kbp genome sequences easily (34, 44).

The purpose of this thesis is to investigate phylogenetical relationship of zebra-borne EHV-1 isolated from zoo animals and molecular biological alterations of the gene lacking a stop codon and the genes related to the pathogenicity of EHV-9.

The study covers the followings:

1. The alteration of non-stop gene ORF19 of EHV-9 mutant strain SP21 was verified at mRNA and protein level by comparison with wild strain EHV-9.

2. Two nucleotide mutations changed amiro acid exist in EHV-9 mutant strain SP21 were repaired by recombination in the strains named SP21-14R and SP21-19R. The virulence of EHV-9, mutant virus SP21, recombinant virus SP21-14R and SP21-19R were investigated *in vitro* and *in vivo*.
3. The genomes of virus isolated from a zebra, an onager, and a gazelle (strains T-616, T-529, and 94-137, respectively) were extracted and sequenced. The phylogenetical relation of the three viruses was characterized.

CHAPTER 1

Non-stop mutation of ORF19 in Attenuated Equine Herpesvirus Type 9

Introduction

Equine herpesvirus 9 (EHV-9) was isolated from a gazelle kept at a zoological garden in Japan, which gazelle died of encephalitis in 1993 (16).

It has been considered that viral gene regulation of EHV-9 should be identical to that of EHV-1. During the lytic cycle of the EHV-1 in culture cells, regulation of gene expression mainly occurs at the transcriptional level involving in immediate-early (IE), early, and late phases (20, 21, 46). For herpes simplex virus type 1 (HSV-1), IE proteins are responsible for regulating viral gene expression during subsequent phases of the replication cycle. Early gene products are synthesized next and are involved in viral DNA synthesis. Late genes encode proteins involved in virion structure and assembly (43). Late genes which require DNA replication for any appreciable accumulation of mRNA are referred to γ2 genes or L2 genes. Some later genes are expressed to a degree in the absence of DNA replication but require DNA synthesis for maximal expression. These genes are referred to γ1 genes or L1 genes (63).

A eukaryotic mRNA contains one open reading frame that consists of a start codon, series of sense codons and a stop codon. Some studies reported non-stop mRNA, which had no stop codon in mRNA. It was reported that the non-stop mRNAs were indicated to be degraded after translation (30, 42). Non-stop mRNA in mammalian cells were degraded fast by the non-stop mRNA decay pathway. 3’ to 5’ exonuclease in the exosome complex promotes the mRNA degradation, and translation is required for the fast decay of non-stop mRNA (10, 30, 42). Hbs1, Dom34, and the exosome-Ski complex were reported to act with the non-stop mRNA decay (5, 42). This degradation is also known for nonstop decay. On the other hand, other researchers reported that the non-stop

mRNA was not significantly reduced and as stable as wild-type mRNA (2, 40, 57). HSV-1 drug-resistant mutant lost the stop condon in thymidine kinase gene greatly decreased the expression level of full-length thymidine kinase protein (40). However, it is still unclear about the function and roles of virus non-stop mRNA and protein in infected cells.

Yamada *et al*. performed serial passaging of EHV-9 using RK-13 cells, which are non-natural host animal cells, and plaque cloning in order to obtain mutant viruses for elucidating which genes were involved in the pathogenicity and virulence of EHV-9 (Yamada, S., PhD Thesis). One of the mutant viruses, designated SP21, formed small plaques in equine cell culture. SP21 was analyzed on growth property in culture cells and pathogenicity and virulence in hamsters. It was found that the virulence of SP21 was lower than that of wild type in the hamster model of EHV-9 infection.

In this Chapter, author determined the complete genome sequence of SP21. Two point mutants were found in ORF14 (Asp230Tyr) and ORF19 (TGA498TTA). The mutation found in ORF19 indicated the non-stop mRNA for ORF19. The objective of this Chapter is to verify the alteration of mRNA and protein translated from the non-stop mRNA of virus in infected cells, and to provide information to study non-stop mRNA decay in mammalian cells.

Materials and Methods

Viruses and cells

EHV-9 wild type and SP21 were used in this chapter. SP21 which is a

mutant virus cloned from EHV-9 seed stock passaged in non-natural host cell rabbit kidney cells (RK13) for 23 times. Culture cells used were fetal equine kidney (FEK), RK13 and bovine kidney (MDBK) cells. FEK cells were cultivated with Dulbecco's minimum essential medium (D-MEM) with low glucose supplemented with 10% fetal bovine serum (FBS) and 100 units/ml penicillin and 100 µg/ml streptomycin. RK13 and MDBK cells were cultivated in minimum essential medium alpha (MEM-α) with 5% FBS and antibiotics.

Genome extraction and sequencing

Viral genomic DNA was extracted as described by Volkening and Spatz (2009) as follows (59). Viruses were inoculated into FEK cells at multiplicity of infection (MOI) 0.1. When 90% of cells showed cytopathic effect (CPE), infected cells were harvested and washed with ice cold phosphate buffered saline (PBS) by centrifugation at 2600 g for 15 min. The supernatant was removed, and the pellet was resuspended in cold permeabilization buffer (320 mM sucrose, 5 mM $MgCl_2$, 10 mM Tris-HCl/pH7.5, 1% triton) and placed on ice for 10 min. Nuclei were pelleted by centrifugation at 2600 g for 15 min at 4°C. Washing the nuclei with the permeabilization buffer twice, the pellet was resuspend in 50 µl nuclei buffer (10mM Tris-HCl/pH7.5, 2mM $MgCl_2$ and 10% sucrose) and mixed with an equal amount of 2x nuclease buffer (40 mM PIPES, pH7.0, 7% sucrose, 20 mM NaCl, 2 mM $CaCl_2$, 10 mM 2-mercaptoethanol and 200 µM PMSF), 3 µl of micrococcal nuclease (Thermo, EU) solution (300 units/µl) and 3 µl of RNaseA (Novagen, South Africa) solution (100 mg/ml). The mixture was incubated at 37°C for 30 min in order to degrade cellular and unpackaged viral

nucleic acids. The reaction was stopped by adding 2.4 µl of 0.5 M EDTA and then added 400 µl of digestion buffer containing 20 mg/ml of protease K. The sample mixture was incubated at 50°C for 18 h. DNA was extracted by phenol and chloroform extraction followed by ethanol precipitation. DNA was finally dissolved in TE buffer (10 mM Tris-HCl, pH8.0, 1 mM EDTA). The small fragments of DNA were removed by two times precipitation using 6.5% polyethylene glycol containing 10 mM $MgCl_2$.

DNA sequencing was examined by using MiSeq(Illumina, USA). The complete genomes were assembled by reference sequence mapping and editing with Consed.

GST-pORF19 fusion protein expression, purification and immunization

Each of the full length wild type ORF19 and mutant ORF19 was amplified by PCR and cloned into pGEX6p-1 vector. The plasmid containing fragment of EHV-9-ORF19 or SP21-ORF19 was introduced in *Escherichi coli* BL21. The protein expression was induced by adding 100 mM Isopropyl β-D-1-thiogalactopyranoside (IPTG) to the final concentration of 400 µM/ml in a log phase culture. After overnight culture at 20°C, bacteria was collected by centrifugation, washed by ice cold STE buffer (10 mM Tris-HCl, pH8.0,150 mM NaCl, 1 mM EDTA) once and resuspend in STE buffer containing lysozyme (100 µg/ml). The suspension was sonicated in ice. Then the sample was centrifuged at 15,000 g for 10 min at 4°C and the sediment was washed with 1% Triton X-100 in PBS twice. The sediment was washed by distilled water twice in order to remove TritonX-100. The sediment containing the fused protein was

resuspended in PBS containing 0.35% Sarkosyl and 5 mM dithiothreitol (DTT). After incubation at room temperature for 30 min, the suspension was centrifuged at 15,000 g for 5 min. The supernatant was transferred to a dialysis tube for dialyzation overnight in PBS at 4℃ . The fusion protein with adjuvant was injected subcutaneously to BALB/C mice for 4 times to produce anti-pORF19 mouse serum. The animal experiments were conducted according to the guidelines for animal experiments in Gifu University and certificated by the Committee of Animal Care and Welfare, Faculty of Applied Biological Sciences, Gifu University.

Confirmation of poly-A tail attachment site

Total RNAs were extracted from EHV-9 or SP21 infected FHK cells at 8 h post infection (p.i). with TRIzol reagent (Life Technologies, USA) according to the manufacturer's instructions and treated with DNase I (Life Technologies, USA). The RNA samples were used to synthesize cDNA with Oligo(dT)20 as primer by ReverTra Ace-α- cDNA synthesis kit (TOYOBO, Japan). The 3'-end fragments of ORF19 in cDNA samples were amplified by PCR using ORF19 specific primer (5'-gcgtaattagctcgctccac-3') and Oligo(dT)20. Sequences of the PCR products were directly determined by Sanger method (Dragon Genomics, Japan).

Immunofluorescence assay

Cells grown on coverslips were subjected to infection or transfection,

prior to be fixed in 4% paraformaldehyde, washed by PBS once, neutralized by 50 mM NH_4Cl and followed by the permeabilization in 0.2% TritonX-100. After blocking in 2% BSA, the cells were stained for indirect immunofluorescence assay. The primary antibodies used in the present study were 200 times diluted anti-pORF19 mouse serum produced in the current study and 200 times diluted anti-EHV-9 rabbit serum received from the lab of Veterinary Pathology, Faculty of Applied Biological Sciences, Gifu University (65). The secondary antibodies used were Alexa Fluor594-conjugated goat anti-mouse IgG (Invitrogen, Japan) and fluorescein isothiocyanate (FITC)-conjugated goat anti-rabbit IgG (MP Biomedicals, USA). After indirect immunofluorescence staining, the coverslips were observed using the LSM700 microscope (Zeiss, Germany).

Western blotting

Samples were dissolved in SDS-PAGE sample buffer and separated by electrophoresis through an SDS-8% polyacrylamide gel and transferred to a sheet of nitrocellulose membrane (MILLIPORE, USA). After blocking with 3% skim milk-0.05% Tween 20 in PBS, the membrane sheet was incubated with anti-ORF19 mouse serum or anti-EHV-9 rabbit serum at a 1:1,000 dilution. After 1 h incubation, the membrane sheet was washed and incubated with streptavidin-horseradish peroxidase conjugated anti-mouse IgG goat serum (ICN Biomedicals, USA) or anti-rabbit IgG goat serum (MP Biomedicals, USA) for another 1 h. The membrane sheet then reacted with Western Blotting Detection reagent mixture (Life Sciences) for 5 mins. Autoradiography films were placed on the membrane for exposure about 5s to 1min.

Quantitation of RNA synthesis

FEK cells in 6 well plates were inoculated with viruses EHV-9 or SP21 at 1 plaque forming unit (pfu) per cell. The virus solution was treated with 1 units/ml of DNase I and 100 ng/ml of RNase A for 30 min on ice before inoculation. Collecting the infected cells at 0, 2, 4, 6, 8 h post-infection, RNA was extracted and reverse-transcribed as descried above. The cDNAs were then used as templates to quantitate the amount of viral RNA with SYBR PrimeScript RT-PCR kit (TaKaRa, Japan) according to the manufacturer's instructions.

Transient transfection assays

pcDNA 3.1(+), pcDNA 3.1(+)-SP21-19 and pcDNA 3.1(+)-EHV-9-19 which were previously prepared, was transfected into RK13 cells with Lipofectamine 2000 (Life Technologies, USA) respectively. The cells were once washed by Opti-MEM medium (Life Technologies, USA), followed by adding the mixture of plasmid and Lipofectamine 2000, and incubated at 37°C for 1h. The mixture was removed, and MEM containing 5% FBS was added. The cells were incubated at 37°C for 24 h prior to testing for gene expression by western blotting or immunofluorescence assay.

Results

Genome sequencing

The genome of SP21 was successfully sequenced. Two point mutations were found in ORF14 and ORF19. The point mutation found in ORF14 changed asparagine at 230 to tyrosine. And the other point mutation in ORF19 changed stop codon TGA to leucine codon TTA. Polyadenylation signal, AATAAA, of ORF19 overlapped with this codon (Fig.1). There was no other mutation affecting amino acid coding changes except these two mutations.

Non-stop virus gene mRNA and poly-adenylation site

The gene ORF19 of SP21 lacking a stop codon was transcribed into non-stop mRNA. To confirm the non-stop mRNA of ORF19 in this study, three series of experiments were carried out. First, RNA was extracted from FEK cells infected with EHV-9 or SP21 at 0, 2, 4, 6, 8 h.p.i. The extracted RNA was reverse-transcribed with Oligo(dT)20 primer and used for quantification of ORF19 mRNA by RT-qPCR. L1 gene ORF73 was used as a reference to evaluate the quantity alteration of mRNA. At 0 h, all Cycle threshold (Ct) values obtained were almost the same and equal to or higher than 37, meaning no detectable PCR products. At 2 h, the amount of mRNA of ORF19 and ORF73 was still less than detectable. After 4 h. p.i., the amount of SP21 ORF19 mRNA was transcribed at the same level as that of the wild type EHV-9, and no significant nonstop decay of the corresponding mRNA was observed (Fig. 2).

In order to obtain ORF19 mRNA 3'-end sequences of EHV-9 and SP21, ORF19 specific primer and Oligo(dT)20 primer were used to amplify the ORF19 cDNA fragment. Both of the PCR products showed the same size (Fig. 3A). The PCR products were sequenced, and the results showed that the Polyadenylation tail was added at the same position, 29 bp post stop codon, unrelated to the presence or absence of the stop codon (Fig. 3B). Therefore, the mRNA of SP21 ORF19 was confirmed to be the non-stop mRNA.

Expression of a full-length of GST-pORF19 fusion protein in bacteria and production of anti-pORF19 serum

ORF19 mRNA without stop condon in SP21 never showed the difference at mRNA transcription level comparing to the wild type EHV-9. For studying the protein expression of non-stop mRNA of virus, the antiserum against pORF19 was produced using GST expression system. The fusion protein product of GST-ORF19 was expressed in bacteria. According to the proteins even not dissolved in tritonX-100, the sonicated bacteria sample was washed by 1% triton X-100 to remove bacteria proteins. The sediment which was dissolved in 0.35% Sarkosyl was analyzed by SDS-PAGE and appeared as a single thick band of the expected size (Approximately 80kDa or 86kDa) in the Coomassie blue stained gel (Fig. 4A). The ORF19 of SP21 elongated to the next stop which was also cloned in pGEX-6p-1 was completely transcribed and expressed in bacteria as expected (Fig. 4A lane2). The purified GST fusion proteins were used to prepare antiserum in mice. The antiserum was tested by western blotting for specificity. As expected, the antiserum reacted with the single polypeptide of the expected

size in RK13 cells transfected with pcDNA3.1-EHV-9-19 lysis (Fig. 4C, lane 1). EHV-9 infected FHK cell lysis (Fig. 4B lane 1), but not mock infected cell lysis and pcDNA3.1 transfected cells lysis reacted with the antiserum(data not shown).

EHV-9 or SP21 infected cells and mock infected cells were prepared for investigating the protein expression by western blotting. pORF19 of SP21 (Fig. 4B lane 2, up) showed smaller band than pORF19 of EHV-9 (Fig. 4B lane 1), although no pORF19 was detected as well as mock infected samples (Fig. 4B lane 3). SP21 infected cell sample reacted with anti-EHV-9 serum has the same band to EHV-9 samples (Fig. 4B lower panel). It was suggested that the pORF19 encoded in SP21 was expressed at the low level in infected cells.

pcDNA 3.1(+)-SP21-19 (the same fragment of ORF19 of SP21 inserted into pGEX-6p-1) or pcDNA 3.1(+)-EHV-9-19 transfected cells were collected at 24 h post-transfected, half of the cell samples used for western blotting to investigate the non-stop protein expression in RK13 cells, the other half cell samples were used for RNAs extraction to confirm the ORF19 of two plasmids transcripted at the same level. The results showed mRNA of ORF19 of SP21 was transcripted at 2 times higher level (Fig. 4D), but proteins expression was significantly lower than wild type. (Fig. 4C lane 1: pcDNA 3.1(+)-EHV-9-19 transfected cells; lane 2: pcDNA 3.1(+)-SP21-19 transfected cells). It suggested that non-stop pORF19 expression was repressed in transient transfection cells.

The location of EHV-9 pORF19 in MDBK cells

The function of EHV-9 pORF19 was unknown. EHV-9 was inoculated

to MDBK cells at MOI 0.05. At 3, 6, 9, 12 h after inoculation, the cells were fixed and reacted with mouse polyclonal anti-pORF19 and secondary anti-mouse IgG conjugated with Alexa Fluor594, following rabbit polyclonal anti-EHV-9 and secondary anti-rabbit IgG conjugated with fluoresceine and examined with a Zeiss confocal microscope. At 3 h after infection, although most virus proteins were found in the nucleus, pORF19 was not detected in both the nucleus and the cytoplasm. The pORF19 was detected around the nucleus and the cytoplasm from 6 h to 12 h after infection (Fig. 5A).

The transient expression of pORF19 in RK13 cells was found in the cytoplasm uniformly and not accumulated around the perinuclear region where pORF19 was observed in infected cells (Fig. 5B).

Discussion

The mutation in SP21 ORF19 changed the stop codon TGA to leucine codon TTA, causing the non-stop mRNA transcription and non-stop protein expression. The non-stop mRNA of ORF19 had the same 3'-tail as that of wild type. The poly-A tail was added 29 bp post stop codon in both wild type and the non-stop ORF19 mRNA. Thus it was confirmed that the mutated ORF19 mRNA was the non-stop mRNA. Some studies showed the non-stop mRNAs degraded by non-stop decay (30, 42). But some studies never observed this phenomenon, and the non-stop mRNA were stable equivalent to the wild type (2, 40, 57). In this Chapter, the author found that the non-stop mRNA of ORF19 was of the same quantity as that of wild type at 2, 4, 6 and 8 h post inoculation. Therefore no non-stop decay was observed for the non-stop ORF19 mRNA.

In this study, the fusion gene consisting of GST and the non-stop gene ORF19 extended to the next stop codon was expressed as the fused protein at the expected size in prokryotic cells (Fig. 4A lane2). On the other hand, pPC-DNA3.1-SP21-19 which encoded the non-stop ORF19 extended to the next stop codon was expressed less than detectable amount in eukryotic cells as shown in Fig. 4C lane 2. Sequencing the non-stop ORF19 indicated that the non-stop ORF19 was not transcribed as the extended mRNA which should include the next stop codon and that the poly-A tail was attached to the same site in both the normal ORF19 mRNA and the non-stop ORF19 mRNA. These data indicated that repression of non-stop protein expression occurred in SP21 infected cells and that even non-stop ORF19 mRNA could be transcribed and modified by the similar manner to the normal mRNA. The repression of non-stop protein expression is also reported by other researchers (40, 42). It is still undefined that the non-stop protein repression is caused by protein expression problem or protein degradation. One study detected the non-stop protein stability by addition of cycloheximide, and not significantly changed during 2 days, suggesting the degradation of non-stop protein was not accelerated *in vivo* (2). But the other report showed that deletion of proteasome assembly factors led to increased non-stop protein level in mammalian cells (5). *Saccharomyces cerevisiae* Ltn1 which was an E3 ubiquitin ligase co-immunoprecipitated with the 19S proteasome (5). The loss of Ltn1 function conferred sensitivity to stress caused by increased non-stop protein production. It means that the non-stop protein administration is affected by the stress to the cell. These discrepanct results led to the hypothesis that cell might feel various stresses to the targets which we used for each study, and induce the variance.

In this Chapter, the author found two point mutations in SP21, the attenuated mutant of EHV-9, by the genome sequencing. One of the mutations in ORF19 caused the non-stop mRNA. The virological significance of the non-stop ORF19 mRNA will be investigated in the next Chapter 2.

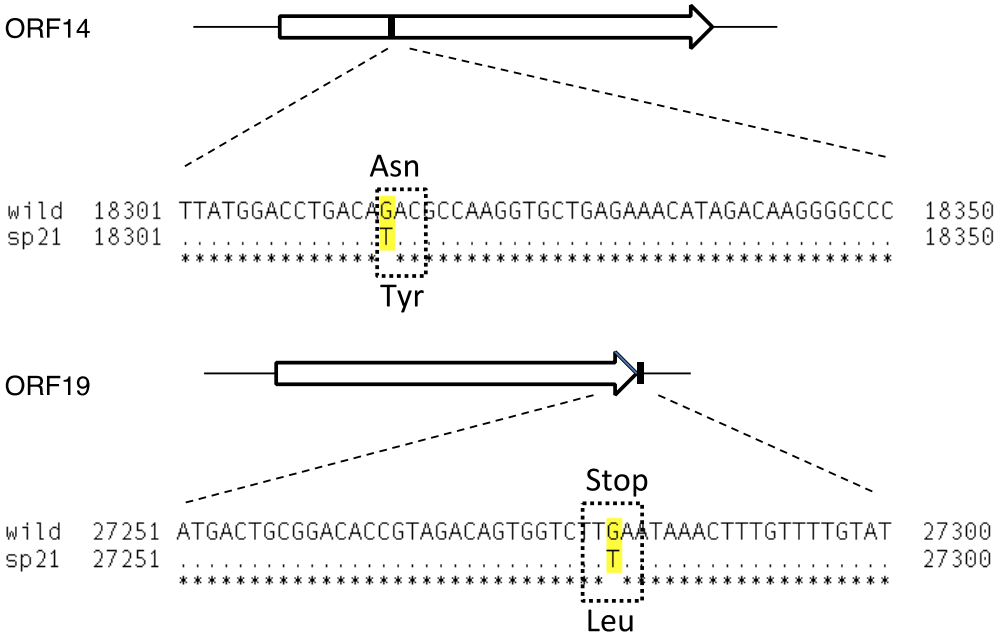

Figure. 1. The mutations in ORF14 and ORF19 of SP21. Reading the full length of genome of SP21, two mutations inducing amino acid changes were found in ORF14 and ORF19. The point mutation in ORF14 changed asparagine (Asn) at 230 to tyrosine (Tyr), and the point mutant in ORF19 changed stop codon (TGA) to leucine codon (TTA).

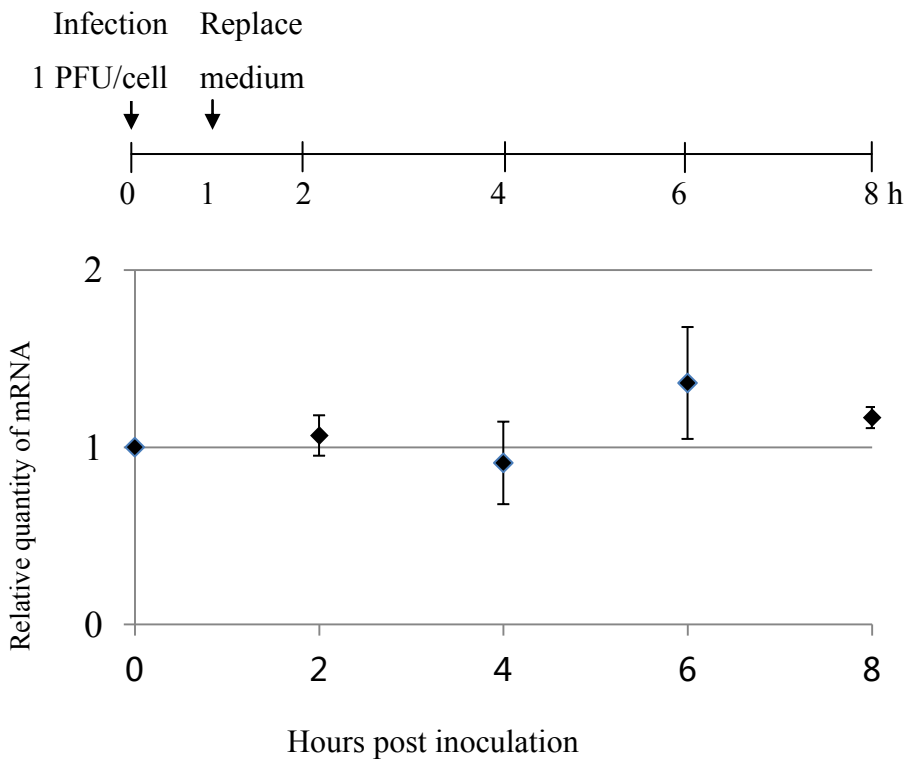

Figure. 2. Relative quantity of non-stop mRNA of ORF19 compared to wild type. The relative quantity value was the ratio between the relative amount of non-stop ORF19 of SP21 normalized with ORF73 of SP21 against the relative amount of ORF19 of EHV-9 normalized with ORF73 of EHV-9. Point at 1 line means mRNA of non-stop ORF19 of SP21 in infected cell kept the same amount to wild type EHV-9, above 1 line means SP21 had more mRNA than wild type at this time, and less than 1 is the opposite. The result is from three independent experiments.

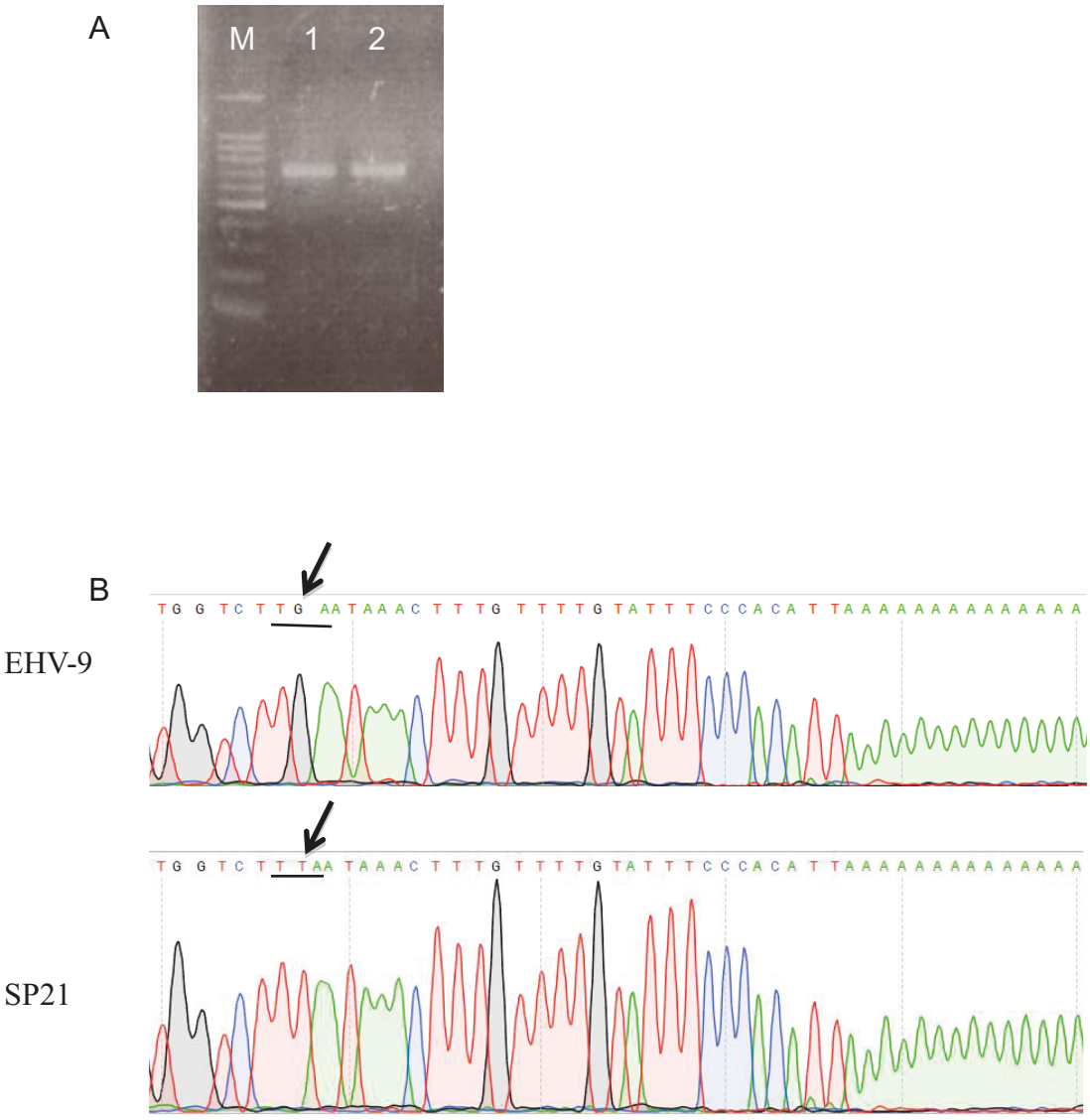

Figure. 3. (A) PCR products corresponding to 3' fragment of ORF19 mRNA of EHV-9 and SP21 (M: 100bp DNA ladder, lane 1:EHV-9, lane 2:SP21).

(B) Sequences of 3' tail of cDNA of ORF19 of EHV-9 and SP21. Arrows indicate the mutation site. Poly-A tail was added at the same position of ORF19 of EHV-9 and SP21.

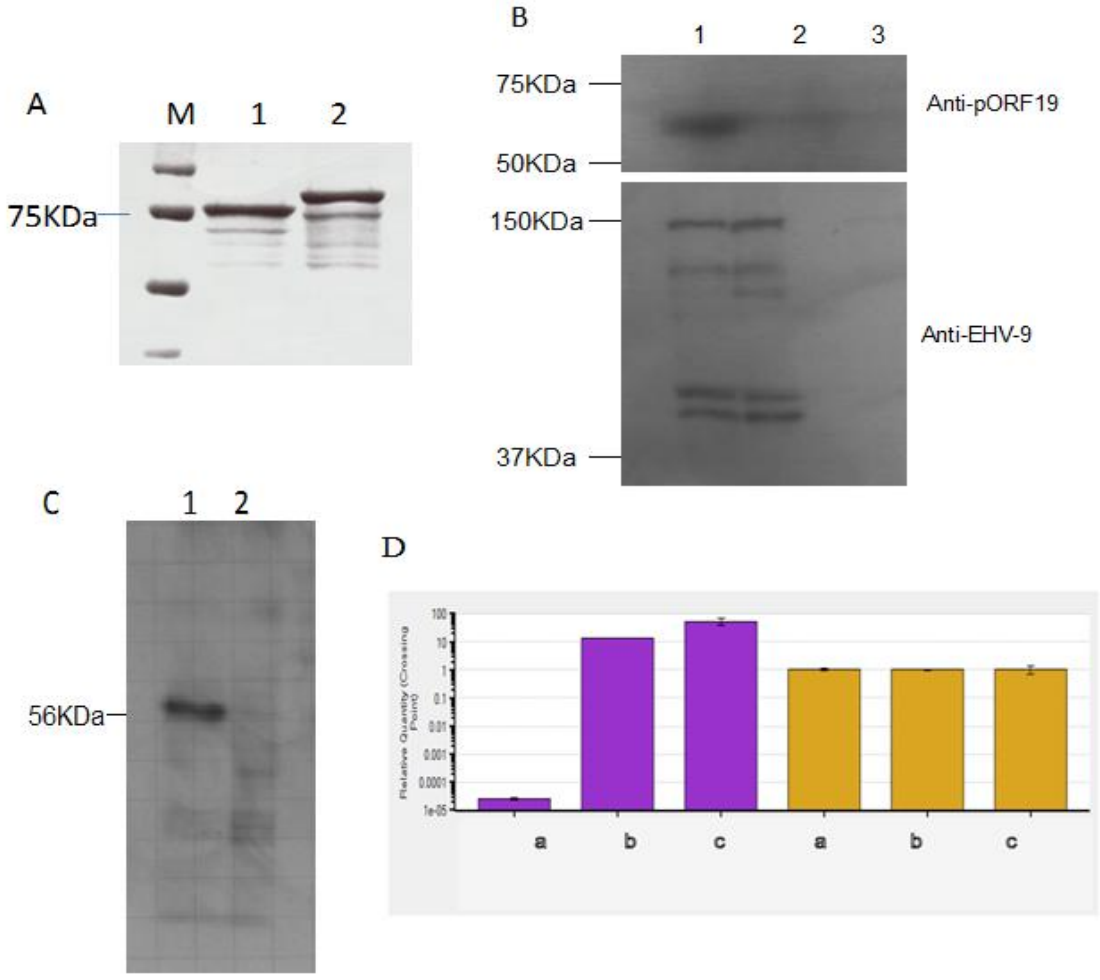

Figure. 4. (A) Expression of GST-ORF19 fusion proteins. GST-pORF19 of EHV-9 (lane 1) and GST-pORF19 of SP21 (lane 2) showed in Coomassie blue-stained gel. (B) FEK cells infected with EHV-9 (lane 1), SP21 (lane 2) and mock (lane 3). Immunoblotting with anti-pORF19 serum and anti-EHV-9 serum. (C) and (D) RK 13 cells were transfected with plasmids of pcDNA 3.1, pcDNA 3.1-EHV-9-19 or pcDNA 3.1-SP21-19. The cells were harvested at 24 hours after transfection. Half cell samples were used to detected pORF19 expression (C. lane1: pcDNA 3.1-EHV-9-19; lane 2 pcDNA 3.1-SP21-19). Half cell samples were used for RNA extraction to check the ORF19 transcription by qRT-PCR. The results were normalized with beta-actin (D. a: pcDNA 3.1, b: pcDNA 3.1-EHV-9-19 c: pcDNA 3.1-SP21-19).

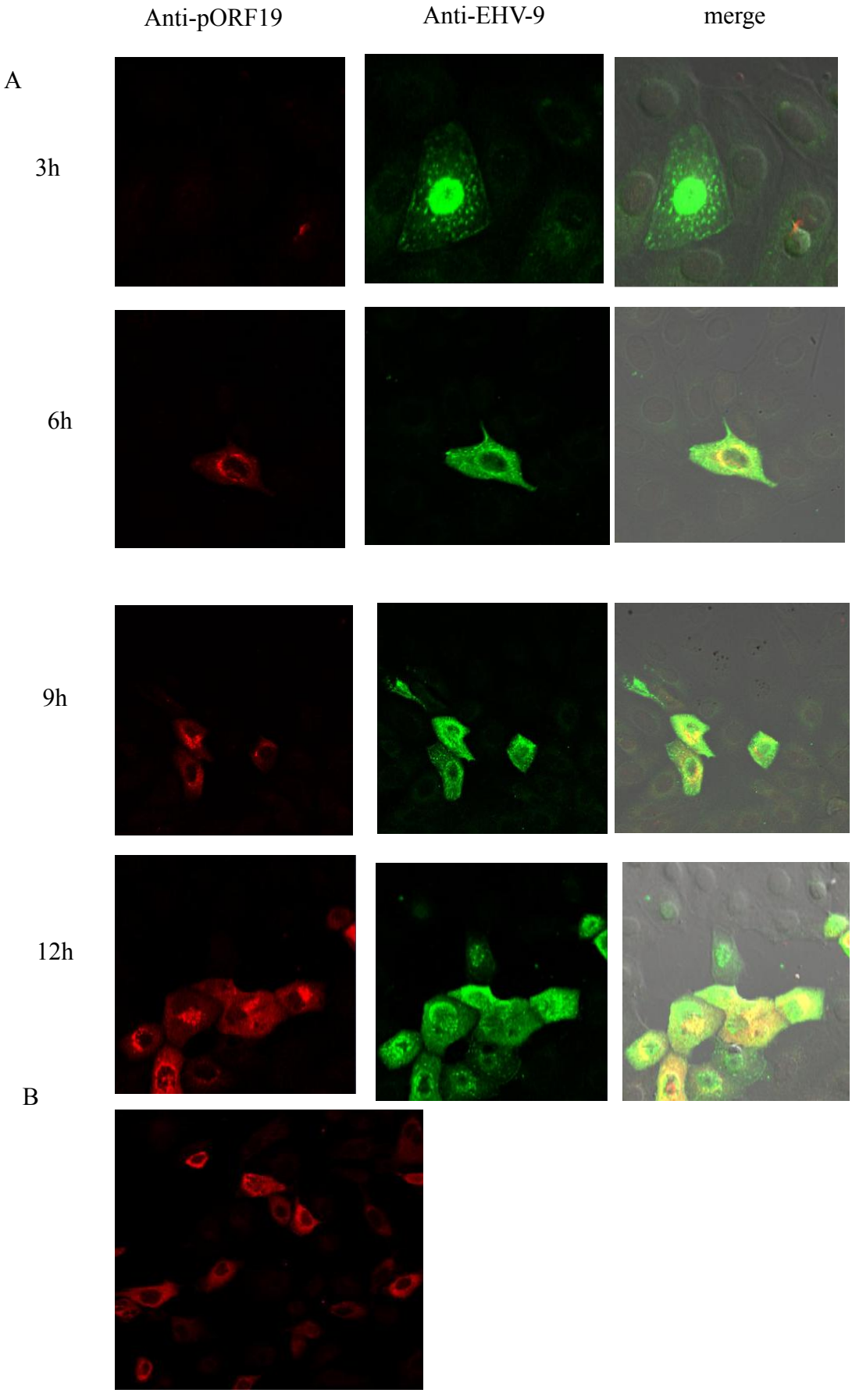
Anti-pORF19
Anti-EHV-9
merge
A
3h
6h
9h
12h
B

Figure. 5. The expression and location of pORF19 in EHV-9 infected cells. (A) EHV-9 infcted MDBK cells were fixed at 3, 6, 9, 12h post-inoculation, and indirectly immunobloted with anti-pORF19 (red) and anti-EHV-9 (green) antiserum. (B) RK13 cells cultured on glass slide, transfected with pcDNA 3.1-EHV-9-19 using Lipofectamine 2000 reagent (Life Technologies, USA), after 24h the cells were fixed, and immunobloted with anti-pORF19 mouse serum and secondary anti-serum Alexa Fluor594-conjugated anti-mouse IgG.

CHAPTER 2

Mutations Associated with Attenuation of Equine Herpesvirus Type 9

Introduction

Equine herpesvirus type 9 (EHV-9) was isolated from an outbreak of epizootic acute encephalitis and sudden death in a herd of Thomson's gazelle (16). EHV-9 is genetically close to equine herpesvirus type 1 (EHV-1) which is the major pathogen to horse caused abortion, respiratory disease and neurological disorder (55). Nugent *et al.* (39) reported one amino acid at 752 of viral DNA polymerase (EHV-1, ORF30) is strongly associated with neuropathogenic versus nonneuropathogenic disease outbreaks based on the variation analysis of EHV-1 isolated from Europe, North and South America, and Australia. EHV-9 has the neuropathogenic maker D_{752} in ORF30. The infection of EHV-9 induced severe neurologic disease in mice, goats, cats, giraffes and marmosets (1, 11, 15, 27, 54, 65, 66).

The previous studies in our laboratory showed that the mutant SP21 had the lower virulence compared to the wild type EHV-9 in the hamster model (Yamada, S., PhD thesis). For searching the factor associated to attenuation, full genome sequencing of SP21 was performed in Chapter 1. Two point mutations were found in ORF14 (Asp230Tyr) and ORF19 (stop498Leu). ORF14 encodes a tegument protein VP11/12 which reacts with VP16 to enhance the expression of immediate-early gene. The lack of VP11/12 was reported not to affect the virus growth in culture cells in HSV-1 (58, 60, 61). The Src family kinase Lck activates VP11/12 of HSV-1 by tyrosine phosphorylation. (48, 60, 61). However, the function of ORF14 in equine herpesviruses is still unknow.

UL41 of HSV-1 (a homologue of Equine herpesvirus 1 ORF19) is a membrane association, virion host shutoff protein (VHS). The VHS suppresses the host cell protein synthesis by degrading cellular mRNA, and other viral

proteins are not required for VHS activity (37, 51, 52). The newly made VHS is sequestered and rendered inactive by another viral protein VP16 or VP22 (45). VHS also enhances translation of viral true late mRNAs, mediates tegument in corporation, and VHS-null mutants were attenuated in the corneas and central nervous system infections in mice. (9, 13, 47). A report verified that pORF19 of EHV-1 did not show any significant VHS activity, but that transiently-expressed ORF19 protein had intrinsic VHS activity comparable to HSV-1 VHS (14). pORF19 of EHV-9 shares 96% amino acid sequence identity with EHV-1 so that pORF19 of EHV-9 should have similar function to that of EHV-1. However, the function of EHV-9 ORF19 was unclear.

In this chapter, two point mutations in ORF14 and ORF19 were repaired to the original nucleotide separately by homologous recombination. Revertant viruses were named SP21-14R and SP21-19R. Experiments were performed to investigate the virulence of EHV-9, SP21, SP21-14R and SP21-19R, and identify the mutation related to the attenuation of SP21.

Materials and Methods

Viruses and cells

EHV-9 was propagated in fetal equine kidney (FEK) cells, assayed for infectivity in rabbit kidney cells (RK13), bovine kidney cells (MDBK) and FEK cells. SP21 which is a mutant virus cloned from EHV-9 by passaged in non-natural host cell RK13 for 23 times and plaque purification was performed three times (Yamada, S., PhD thesis). FEK and immortalized fetal horse kidney

(FHK3.1) cells were cultivated with Dulbecco's minimum essential medium (D-MEM) with low glucose supplemented with 5-10% fetal bovine serum (FBS), 100 units/ml penicillin and 100 µg/ml streptomycin. RK13 and MDBK were grown in minimum essential medium alpha (MEM-α) with 5% FBS.

Construction of the recombinant plasmids

EHV-9 DNA was used as template to amplify fragments of approximately 4,000 bps in length for ORF14 and ORF19 recombination. The PCR was carried out by using PrimerSTAR Max DNA Polymerase (TAKARA BIO INC, Japan). Reaction mixture contained 25 µl of 2x PrimerSTAR Max Premix, 1.2 µl of each primer, 19.6 µl of distilled water and 3 µl of virus supernatant which was boiled for 10 min before used as the template solution. PCR program consisted of denaturing at 98°C for 10 second, annealing at 67°C for 5 second and extension at 72°C for 45 second. The PCR products were ligated to the linearized vector pUC19 DNA using T4 ligase (Promega, USA). Each of pUC19-14 and pUC19 -19 was used as a template for PCR. Primers used for PCR were ORF14-F 5'-AACTCCATATATGGGtaagctggtcggtatatggagtggc-3', ORF14-R 5'-TGTATCTTAACGCGTggacgtcccactcgtggaagagcaa-3', ORF19-F 5'-AACTCCATATATGGGagtgtaagctttacgcgcggaaagt-3' and ORF19-R 5'-TGTATCTTAACGCGTaagtggtatagctgtaaagtgtagg-3'. Each primer contained 15 bp sequence homologous to pCMV-EGFP, which sequences were shown in uppercase. The amplification program consisted of 98°C for 10 second, 5 cycles of 57°C for 15 second, 72°C for2 min followed by 30 cycles of 98°C for 5 second, 63°C for 5 second, 72°C for 2 min. The PCR product was digested with

the restriction enzyme DpnI to remove circular plasmid DNAs. A green fluorescent protein expression cassette was amplified using pEGFP-C1 as a template and inserted into each of pUC19-14 and pUC19-19 DNA with Infusion kit (TaKaRa, Japan) according to the manual. The resulting plasmids designated as pUC19-14, pUC19-14GFP, pUC19-19 and pUC19-19GFP were used for recombination (Fig. 6).

Construction of revertant viruses SP21-14R and SP21-19R

FHK3.1 cells in 35mm dishes were infected with SP21 at MOI 0.1. After adsorption for 1 h, cells were washed once by Opti-MEM medium (Life Technologies, USA), and transfected by 4 μg of linearized pUC19-14GFP or pUC19-19GFP DNA by the method described at the section of transient transfection assays in last chapter. 1 h later, Lipofectamine 2000 and plasmid DNA mixture were removed. The transfected cells were covered by fresh medium D-MEM containing 5% FBS. When 90% of the cells showed CPE, the supernatant was collected.

Appropriate dilutions of the virus supernatant were inoculated into FHK cells. After 1h of adsorption, cells were covered by Eagle's medium (NISSUI, Japan) containing 5% FBS and 1.5% carboxymethylcellulose. 36 h later, the plaques showing green fluorescence were selected under fluorescent microscopy. Recombinant virus SP21-14GFP or SP21-19GFP was plaque purified until all plaques showed green fluorescence.

To construct revertant viruses SP21-14R and SP21-19R, each of recombinant viruses SP21-14GFP and SP21-19GFP was used to infect to FHK3.1

cells. After 1 h adsorption, 4 µg linearized pUC19-14 or pUC19-19 DNA was transfected. The supernatant was collected, when 90% cells showed CPE. Plaques without green fluorescence were picked up and plaque purification was examined untill all plaques did not show green fluorescence. These processes were showed in fig. 7. SP21-14R and SP21-19R viruses were confirmed by genome sequencing using MiSeq (Illumina).

Cycleave polymerase chain reaction (PCR)

The Cycleave PCR method is a useful way to detect a point mutation. The author used this method to divide EHV-9, SP21, SP21-14R and SP21-19R. The primers and probes of Cycleave PCR were designed on line (http://www.takara-bio.co.jp/prt/snps/intro.htm). The reaction mixture contained 12.5 µl of 2X Cycleave PCR reaction mix (Takara, Japan), 0.5 µl of forward and reverse primers (final concentration of 0.2 µM), 1 µl of FAM and ROX probe (final concentration of 0.2 µM) and 2 µl of virus supernatant solution as a template, up to 25 µl with distill water. The mixture was subjected to the reaction at 95°C for 2 min, 45 cycles of 95°C for 5 s, 52°C for 10 s, and 72°C for 20 s by Thermal Cycler Dice Real Time System (Takara, Japan).

Genomic DNA extraction

Viruses SP21-14R and SP21-19R were propagated in FHK cells. When 90% cells showed CPE, the supernatant was collected and centrifuged at 2,600 g for 15 min to remove the cells and nuclei. Then the supernatant was centrifuged

at 25,000 rpm (Hitachi, Japan) for 1 h. The sediment containing virions was resuspended in 100 µl of nuclei buffer (10mM Tris-HCl/pH7.5, 2mM $MgCl_2$ and 10% sucrose) and then mixed with an equal volume of 2x nuclease buffer (40 mM PIPES, PH7.0, 7% sucrose, 20 mM NaCl, 2 mM $CaCl_2$, 10 mM 2-mercaptoethanol and 200mM PMSF), 1 µl (300 units) of micrococcal nuclease solution and 1 µl (100mg/ml) of RNaseA solution. The mixture was incubated at 37°C for 30 min to degrade cellular and unpackaged viral nucleic acids. The reaction was stopped by adding 2.4 µl of 0.5 M EDTA, then added 400 µl of digestion buffer containing 5 µg of protease K (TaKaRa). The sample mixture was incubated at 50°C for 18 h. DNA was extracted by phenol and chloroform extraction followed by ethanol precipitation. DNA was finally dissolved in a small volume of TE buffer.

Western blotting

The superantant of infected cell culture was collected and centrifuged at 2,600 g for 15 min, and the superantant was centrifuged at 25,000 rpm (Hitachi, Japan) for 1 h, the sediment containing virions was resuspended in PBS. Virion samples were mixed with SDS-PAGE sample buffer and separated by electrophoresis through an SDS-8% polyacrylamide gel and transferred to a sheet of nitrocellulose membrane (Millipore, USA). After blocking with 3% skim milk-0.05% Tween 20 PBS, the membrane sheet was incubated with anti-ORF19 mouse serum or anti-VP22 rabbit serum at a 1:1,000 or 1:10000 dilutions. After 1 h incubation, the membrane sheet was washed and incubated with streptavidin-horseradish peroxidase conjugated anti-mouse IgG goat serum

(ICN Biomedicals, USA) or anti-rabbit IgG goat serum (MP Biomedicals, USA) for another 1 h.

Plaque size measurement

For the plaque size measurement, FHK3.1 cell monolayer in 6-well plates was inoculated with viruses. At 3 days p.i., the cells were fixed and stained by crystal violet solution (0.2% crystal violet, 10% methanol, 10% formalin and 2% sodium acetate). The diameters of approximately 100 randomly selected plaques were measured by using ImageJ software (http://rsbweb.nih.gov/ij/).

Viral growth kinetics

FHK cells in 24-well plate were infected by EHV-9, SP21, SP21-14R or SP21-19R at a MOI of 0.01. After 60 min adsorption, the virus solution was removed. The cells were washed with D-MEM once and maintained with fresh D-MEM. Supernatant was collected at 0, 12, 24, 36, 48, and 60 h p.i.. Extracellular titers of each virus sample were determined by plaque assay as described above.

Animal experiments

Three-week-old specific pathogenic free (SPF) male Syrian hamsters (SLC, Shizuoka, Japan) were used in this study. All experiments were conducted according to the guidelines for animal experiments in Gifu University and

certificated by the Committee of Animal Care and Welfare, Faculty of Applied Biological Sciences, Gifu University. Every five hamsters per group were anesthetized by hydrochloric acid-medetomidine (Nippon Zenyaku Kogyo, Japan) with 0.01 mg in 100 µl of physiological saline per hamster, then intranasally inoculated with 50 µl of virus suspension containing 1 x 10^3 and 1 x 10^2 pfu. For the mock infection group, the same volume of D-MEM was inoculated. In the next two weeks, body weight and clinical signs were observed every day.

Results

Construction of recombinant viruses SP21-14R and SP21-19R

The genome sequences showed two point mutations in ORF14 and ORF19 as described in Chapter 1. The point mutation in ORF14 changed GAC to TAC (Asp230Tyr) and point mutation in ORF19 changed stop codon TGA to leucine codon TTA (Fig. 1).

Which mutation played a role in the attenuation of SP21 was confirmed. Each point mutation in ORF14 and ORF19 was repaired to the original sequence by homologous recombination. Plasmids pUC19-14, pUC19-14GFP, pUC19-19 and pUC19-19GFP were used for homologous recombination (Fig. 7).. The desired recombinant viruses were confirmed to be repaired by cycleave PCR. Each of SP21-14R and SP21-19R virus genome sequences was read to confirm that the target mutation site was reverted to the wild type sequence without any additional mutations. The desire viruses SP21-14R and SP21-19R were obtained

without any other additional amino acid changes.

Investigation of pORF19 in virions

The author analyzed virion preparations to investigate the incorporation of pORF19 into virions. The virions of SP21, SP21-14R and SP21-19R were compared with a dilution series derived from EHV-9 virions. Due to the sediment containing the mature virions and inmature virions, VP22 encoded by ORF11 was selected as an internal control protein. pORF19 in SP21 virion was 20% of that in EHV-9. On the other hand, pORF19 in SP21-14R and SP21-19R were 55% and 100% of that in EHV-9, respectively (Fig. 8).

Virological properties of SP21-14R and SP21-19R in cell culture

To evaluate the influence of point mutations on virological properties, plaque sizes formed by EHV-9, SP21, SP21-14R and SP21-19R were compared. Plaques formed by SP21-19R were smaller, approximately 50% of EHV-9 (Fig. 9). In contrast, plaques formed by SP21-14R were larger than those by SP21 and EHV-9, approximately 200% of EHV-9 (Fig. 9). It was suggested that the point mutant in ORF14 affected the plaque size which might be related to cell-to-cell spreading and that the mutation in ORF19 might be suppressed the spreading of EHV-9 between cells.

The viral replication of EHV-9, SP21, SP21-14R and SP21-19R were assessed by the multi-step growth experiments. Inoculating EHV-9, SP21, SP21-14R or SP21-19R to FHK cells at 0.01 pfu per cell, cultivated supernatants

were collected at 0, 12, 24, 36, 48, 60 h post-inoculation. The extracellular viral titers were measured by plaques formation in MDBK cells. The results showed that SP21 and SP21-14R replications were similar to the wild type virus replication. In contrast, extracellular titer of SP21-19R was approximately 50-fold lower than those of wild type virus (Fig. 10). It was suggested that the point mutation in ORF14 was related to the virus growth efficiency in cell culture.

Virulence of EHV-9 wild type, SP21 and revertants in hamsters

To compare the virulence of EHV-9, SP21, SP21-14R and SP21-19R, hamsters were inoculated with the viruses intranasally. The mean body weight of hamsters inoculated with SP21 or SP21-14R decreases on 5 and 6 days post-inoculation and increased again later. The hamsters inoculated with EHV-9 and SP21-19R were losing their body weight and died (Fig. 11). Hamsters inoculated with 10^2 and 10^3 of EHV-9 and SP21-19R started to show hypersalivation, eye mucus, convulsion and hypersensitive reaction symptom and loss weight on 4 days post-inoculation (Table 1). On the other hand, hamsters inoculated with SP21 and SP21-14R started to show neurological symptoms and lost their body weight on 5 days post-inoculation and then they were recovered, although one hamster inoculated with 10^3 PFU of SP21 showed hypersalivation and eye mucus on 5 days post-inoculation and died on 13th day (Table 1).

Discussion

In this Chapter, revertant viruses of SP21-14R and SP21-19R were constructed, and their biological characteristics *in vitro* and *in vivo* were investigated with EHV-9 and SP21.

Small plaque formation and lower virus growth rate of SP21-19R indicated the mutation in ORF14 affected the virus replication in cell culture (Fig. 9 and 10). However, pORF14 might not play any role in virulence of EHV-9 in hamster infection. On the other hand, VP11/12 enconded by HSV-1 UL46, a homologue of EHV-9 ORF14, null mutation did not affect the viral replication (67), and the function of VP11/12 have not been clearly defined (48, 61). Discrepancy of these results on pORF14 should be investigated furthermore.

SP21 and SP21-14R showed low virulence in hamster model, and SP21-19R recovered the virulence equivalent to the wild type EHV-9. These results suggested that mutation in ORF19 is strongly associated with the attenuation of SP21. It was reported that VHS-null mutants of HSV-1 were attenuated in the corneas and central nervous system infection of mice (47). On the other hand, virions of SP21-14R had less pORF19 than those of the wild type and more pORF19 than those of SP21 (Fig. 8). The virulence might not be affected by the amount of pORF19 in virions. The most straigtforward explanation for this finding is that non-stop pORF19 could be expressed at some amount but lost the activity in infected cells of hamsters. Although the present data indicated that pORF19 might play a role in virulence expression of EHV-9 in hamsters, the molecular mechanism of pORF19 in the virulence expression could not be clarified.

In this chapter, the author identified the mutation in ORF14 association with virus replication in cell culture and demonstrated ORF19 related to virus pathogenicity. The results should be useful in future attempts to understand the pathogenicity of EHV-9 at the molecular level.

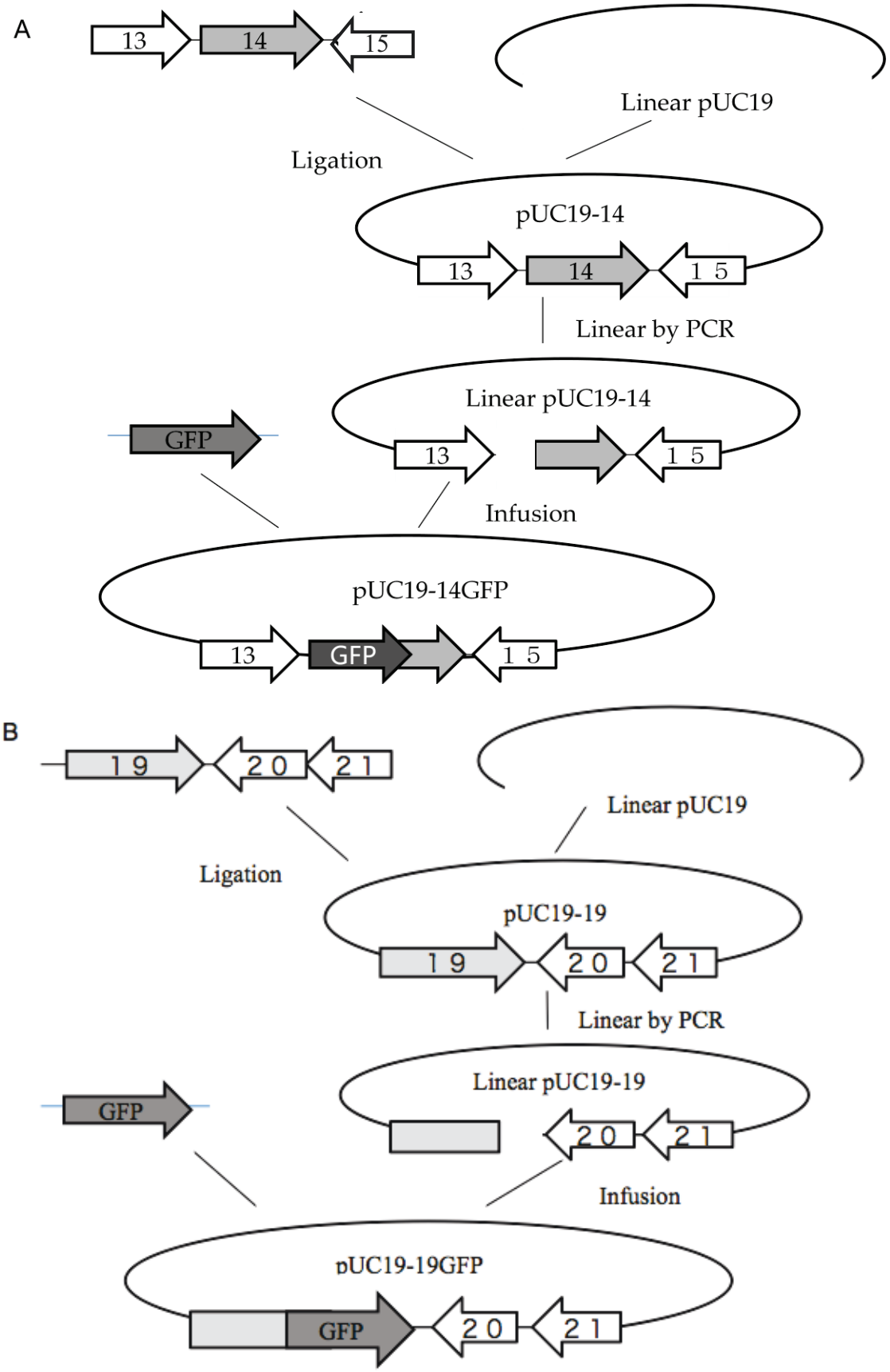
A
13
14
15
Linear pUC19
Ligation
pUC19-14
13
14
15
Linear by PCR
Linear pUC19-14
GFP
13
15
Infusion
pUC19-14GFP
13
GFP
15
B
19
20
21
Linear pUC19
Ligation
pUC19-19
19
20
21
Linear by PCR
Linear pUC19-19
GFP
20
21
Infusion
pUC19-19GFP
GFP
20
21

Figure. 6. Construction of plasmids pUC19-14, pUC19-14GFP, pUC19-19, and pUC19-19GFP for recombination. (A) A fragment containing ORF13, ORF14 and ORF15 of EHV-9 was amplified by PCR and inserted into the linearized pUC19 plasmid. The plasmid pUC19-14 was linearized by PCR. A fragment of GFP and CMV promoter was amplified from pEGFP-C1 and inserted into the linearized pUC19-14. (B) pUC19-19 and pUC19-19GFP were constructed in the same manner to pUC19-14 and pUC19-14GFP.

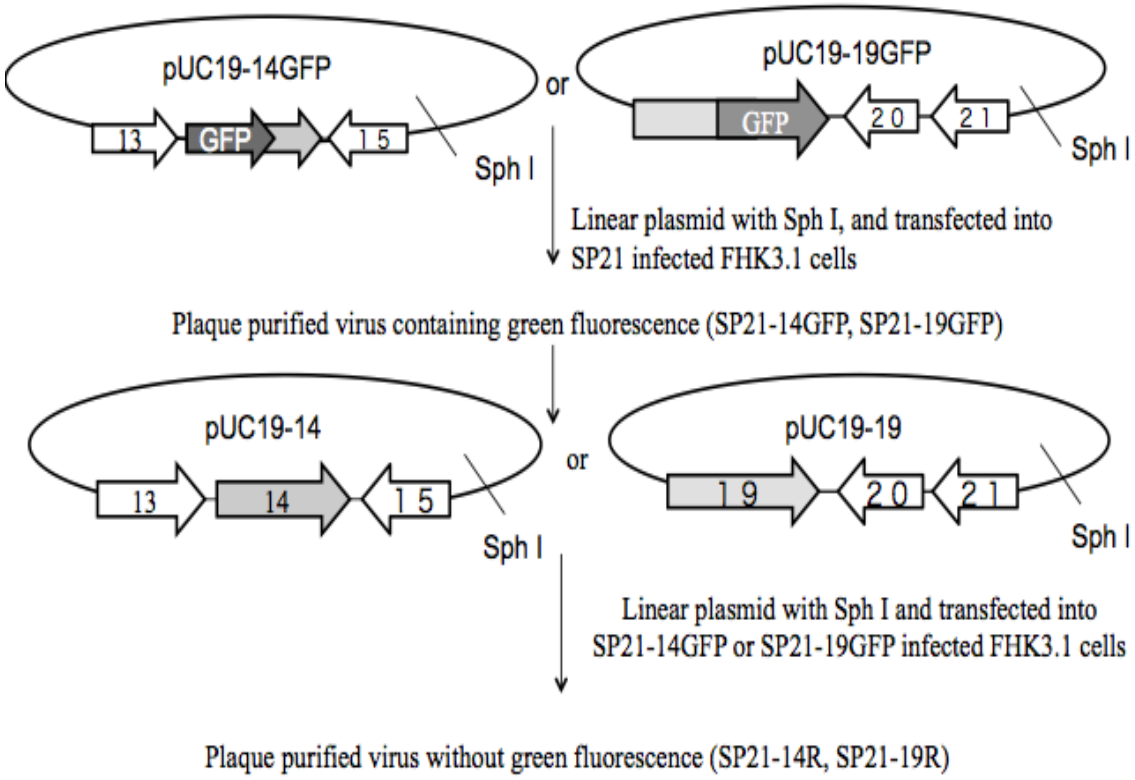

Figure. 7. Construction of recombinant viruses SP21-14R and SP21-19R. Plasmids pUC19-14GFP or pUC19-19GFP was linearized by restriction enzyme Sph I, and transfected into SP21 infected FHK 3.1 cells. The viruses containing green fluorescence (SP21-14GFP, SP21-19GFP) were selected and plaque-purified. Then the linearized pUC19-14 or pUC19-19 was transfected in SP21-14GFP or SP21-19GFP infected FHK 3.1 cells. The viruses (SP21-14R, SP21-19R) without green fluorescence were selected and plaque-purified.

A

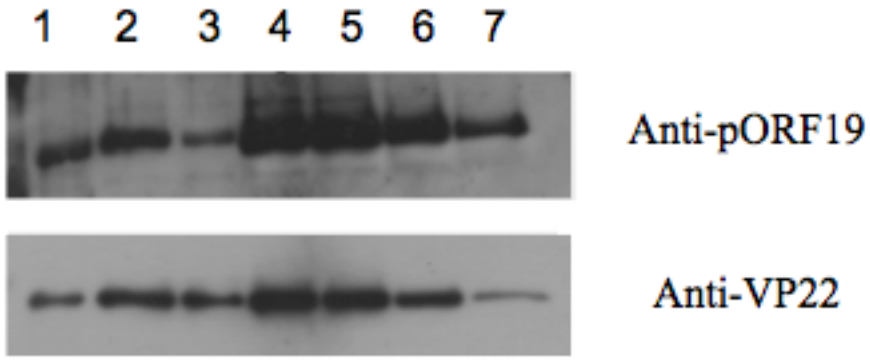

B

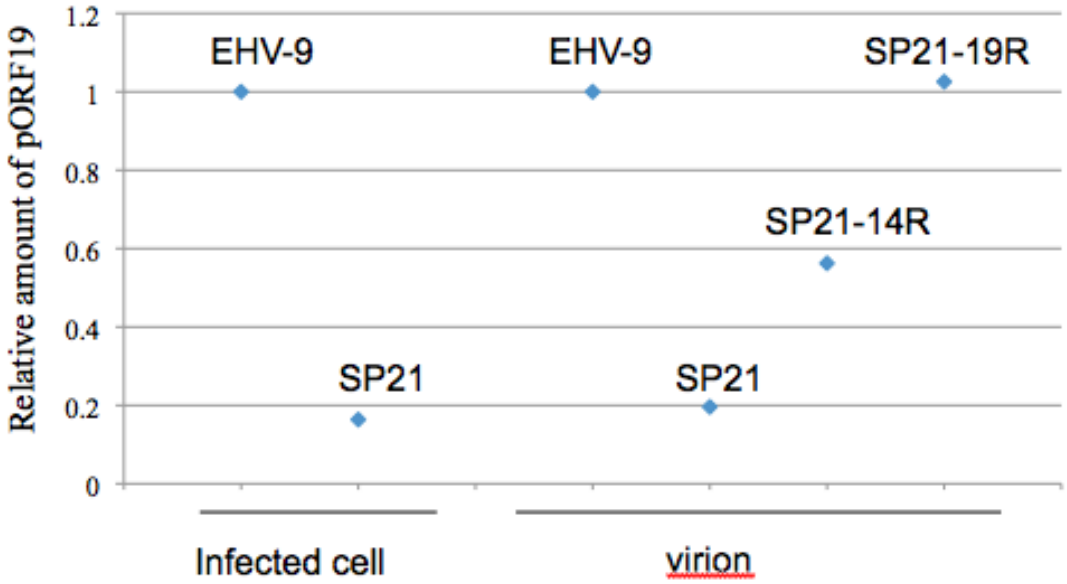

Figure. 8. (A) SP21-19R (lane 1), SP21-14R (lane 2), SP21 (lane 3), EHV-9 (lane 4), 80% EHV-9 (lane 5), 40% EHV-9 (lane 5), 20% EHV-9 (lane 6) virions were separated in 8% SDS-polyacrylamide gel and immunoblotting with anti-pORF19 mouse serum or anti-VP22 rabbit serum as reference. (B) The relative amount of pORF19 in SP21 infected cell (left), SP21, SP21-14R, SP21-19R virions (right). EHV-9 value was defined as 1. The result is based on the analysis with Image J software.

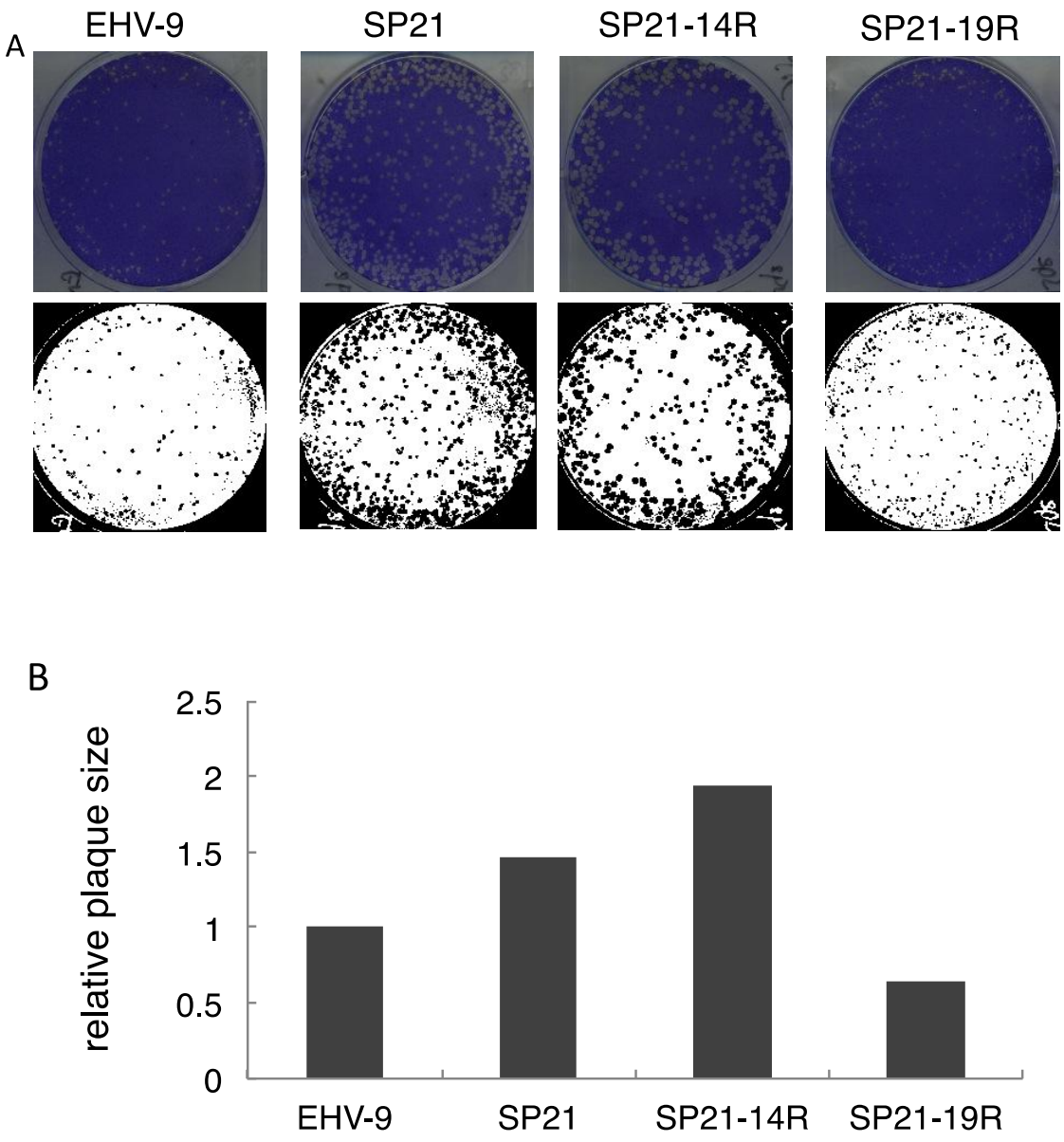

Figure. 9. (A) Plaques formed by EHV-9, SP21, SP21-14R and SP21-19R in FHK 3.1 cells. (B) The relative plaque sizes of EHV-9, SP21, SP21-14R and SP21-19R in FHK 3.1 cells. Two independent experiments showed the same result.

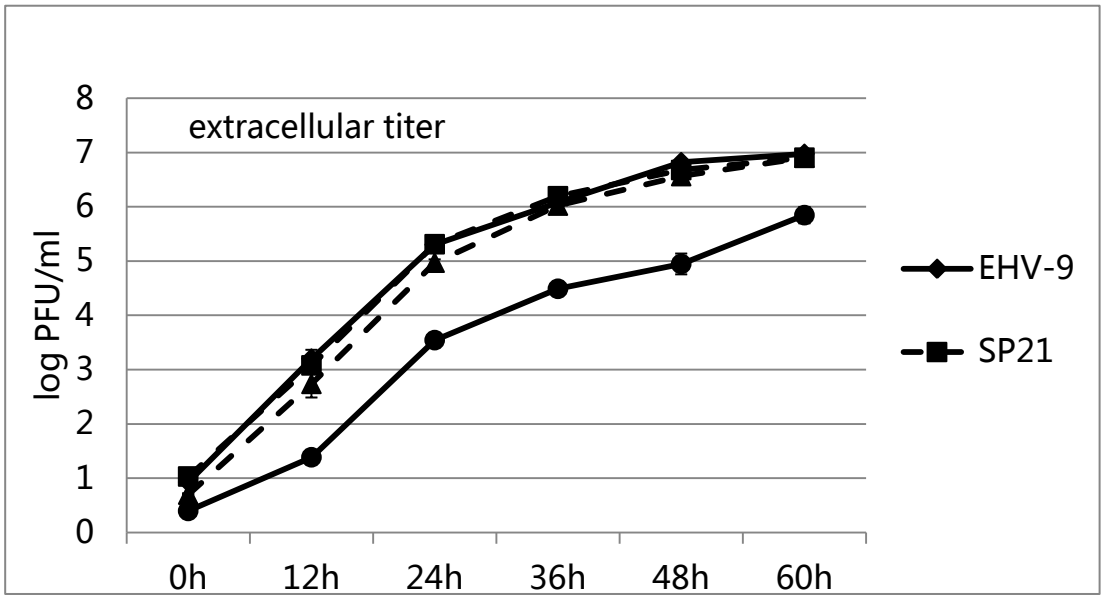

Figure. 10. Multi-step growth curves of EHV-9, SP21, SP21-14R and SP21-19R in FHK cells. FHK culture media was collected at 0, 12, 24, 36, 48, 60h post-inoculation. Virus titration was determined by plaque forming in MDBK cells.

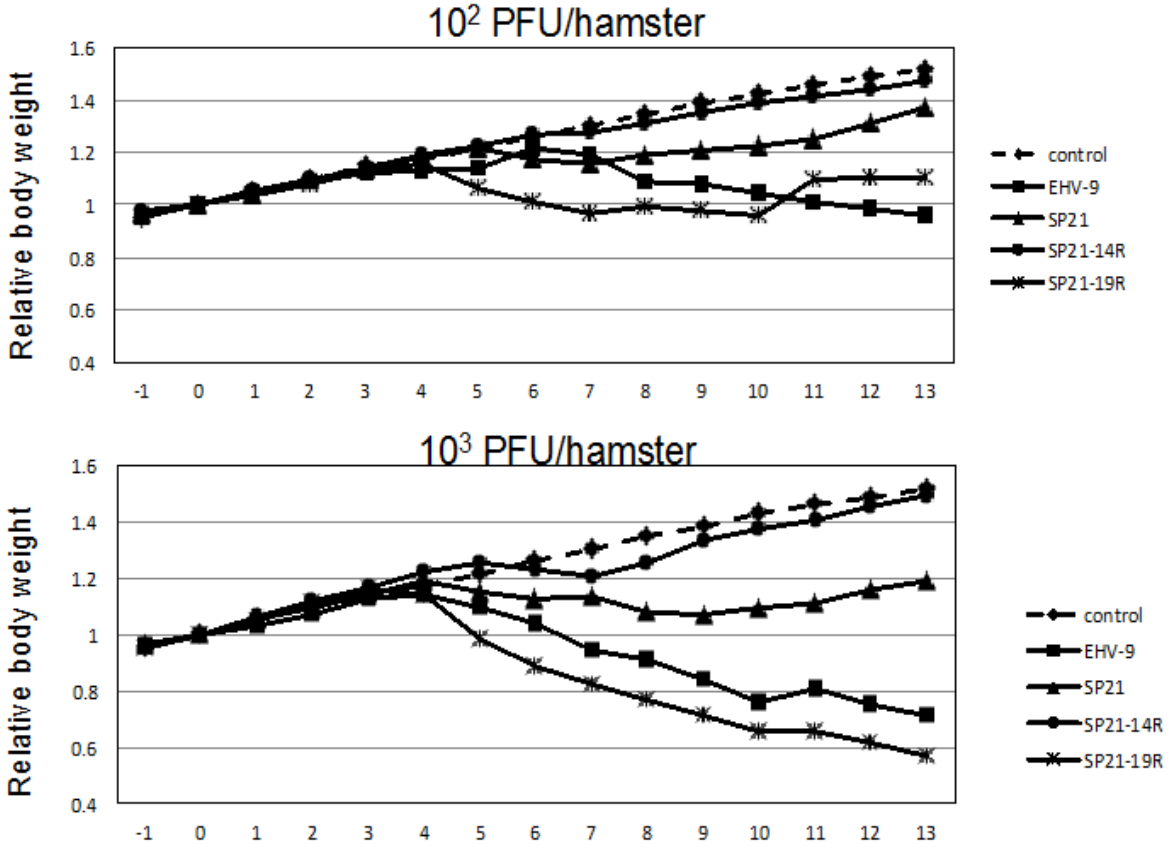

Figure. 11. Relative body weight of hamsters infected with EHV-9, SP21, SP21-14R and SP21-19R. Hamsters were infected with 50 µl of EHV-9, SP21, SP21-14R or SP21-19R containing 10^2 or 10^3 PFU or D-MEM as a control. Body weight was measured every day until 13 days post inoculation. The result is average weight of each day compared to the average weight at 0 day.

Table 1 . The numbers of hamster inoculated with EHV-9, SP21, SP21-14R and SP21-19R showed symptom

virus dose (PFU/ hamster)		Day post-inoculation													
		0	1	2	3	4	5	6	7	8	9	10	11	12	13
10^2	EHV-9	-	-	-	-	1/5	1/5*	1/4	2/4	3/4*	2/3	2/3	2/3	2/3	2/3
	SP21	-	-	-	-	-	-	2/5	2/5	2/5	1/5	2/5	-	-	-
	SP21-14R	-	-	-	-	-	-	1/5	1/5	1/5	-	-	-	-	-
	SP21-19R	-	-	-	-	1/5	3/5	3/5	3/5*	2/4	2/4	2/4*	1/3	1/3	1/3*
10^3	EHV-9	-	-	-	-	2/5	2/5	4/5	5/5*	4/4*	2/2	2/2*	1/1	1/1	1/1
	SP21	-	-	-	-	-	2/5	2/5	4/5	4/5	3/5	2/5	1/5	1/5	1/5*
	SP21-14R	-	-	-	-	-	1/5	3/5	4/5	1/5	-	-	-	-	-
	SP21-19R	-	-	-	-	3/5	5/5	5/5	5/5	5/5	5/5	5/5*	3/3	3/3*	2/2*

- no any symptom or weight decrease

* hamster died

CHAPTER 3

Zebra-borne Equine Herpesvirus Type1 isolated from Zebra(T-616), Onager (T-529) and Thomson's Gazelle (94-137)

Introduction

Equine herpesvirus type 1 (EHV-1; genus Varicellovirus, subfamily alphaherpesvirinae) has been isolated from zebras and other zoo animals (1, 22, 29, 36, 64). Especially the one isolated from zebras has been focused as an emerging agent in zoo animals. The EHV-1 associated with zebras has been called as zebra-borne EHV-1 (1). Zebra-borne EHV-1 has been isolated from wild equids kept in zoological gardens. EHV-1 T-529 was isolated from a Persian onager (*Equus hemionus onager*) fetus in February 1984 [16]. Associated with this case, a 9-month-old male plains zebra (*Equus quagga burchelli*), which was kept in a pen adjacent to the onagers, developed illness a week after the onager abortion. In October 1984, a Grevy's zebra (*Equus grevyi*) at the Lincoln Park Zoo in Chicago aborted a fetus from which EHV-1 T-616 was isolated (64). Systemic infection by EHV-1 in a Grevy's zebra stallion was also reported in 1998 (6). EHV-1 has been isolated from non-equine species including camels, antelopes, cattle, fallow deer, alpacas, llamas, and Thomson's gazelle (*Eudorcas thomsoni*) from which EHV-1 94-137 was isolated (29). A polar bear (*Ursus maritimus*), named Jerka, kept in a zoo in Berlin died from acute encephalitis (22) and a strain of zebra-borne EHV-1 was subsequently isolated from it. The nucleotide sequence analysis of the Pol gene (ORF30) in EHV-1 gene nomenclature (55), a homologue of herpes simplex virus 1 (HSV-1 UL30) in this virus indicated that the virus was a recombinant virus between EHV-1 and equine herpesvirus type 9 (EHV-9), which was isolated from an epizootic encephalitis of Thomson's gazelles kept in a zoo in Japan (16, 17). A similar zebra-borne EHV-1 was detected in an Indian rhinoceros (*Rhinoceros unicornis*) affected by severe neurological disease (1). All of these cases were

reported to be associated with zebras (*E. q. burchelli* and *E. gravyi*) kept at places close to the affected animals.

In the present study, we determined the full genome sequences of three zebra-borne EHV-1s isolated from a zebra, an onager and a gazelle (strains T-616, T-529 and 94-137, respectively). We have reported the phylogenic relatedness among the three viruses based on the nucleotide sequences of the genes for glycoproteins B (ORF33, a homologue of HSV-1 UL31), G (ORF70, a homologue of HSV-1 US4), I (ORF73, a homologue of HSV-1 US7) and E (ORF74, a homologue of HSV-1 US8), and teguments including ORF8 (a homologue of HSV-1 UL51), ORF15 (a homologue of HSV-1 UL45), ORF68 (a homologue of HSV-1 US2) (18, 25). Our results in the present study indicate that the zebra-borne EHV-1 forms an independent group of viruses phylogenetically and that the zebra-borne EHV-1 suspected to have killed Jerka is not a recombinant virus.

Materials and Methods

Viruses and cells

T-529 and T-616 were kindly provided by Dr. G. P. Allen (University of Kentucky, USA) and 94-137 was kindly provided by Dr. Kennedy (University of Tennessee, USA). The three strains of zebra-borne EHV-1 were cultured in fetal equine kidney (FEK) cells. Cells were grown in minimum essential medium alpha (Wako, Japan) supplemented with 100 IU/ml penicillin, 100 µg/ml streptomycin and 10% fetal bovine serum (FBS).

Herpesvirus genome DNA extraction

The genome DNA of viruses isolated from zebra, onager and gazelle were extracted from infected FEK cells by a protocol reported by Volkening and Spatz as follows (59). Viruses were inoculated into FEK cells at MOI 0.1. When 90% cells showed CPE, infected cells were harvested by scraper and washed with cold PBS by centrifuged at 2600 x g for 15 min. The supernatant was removed and the pellet was resuspended in cold permeabilization buffer (320 mM sucrose, 5 mM $MgCl_2$, 10 mM Tris-HCl, pH7.5, 1% Triton-X100) and placed on ice 10 min. Nuclei were pelleted by centrifugation at 2600 x g for 15 min at 4°C。Washing the nuclei with the permeabilization buffer twice, the pellet was resuspend in 50 µl nuclei buffer (10mM Tris-HCl/pH7.5, 2mM $MgCl_2$ and 10% sucrose) and mixed with an equal amount of 2x nuclease buffer (40mM PIPES, pH7.0, 7% sucrose, 20 mM NaCl, 2 mM $CaCl_2$, 10mM 2-mercaptoethanol and 200 µM PMSF), 3 µl (300 units/µl) of micrococcal nuclease and 3 µl (100 mg/ml) of RNase A. The mixture was incubated at 37°C for 30 min to degrade cellular and unpackaged viral nucleic acids. The reaction was stopped by adding 2.4 µl of 0.5M EDTA, then added 400 µl of digestion buffer containing 2.5 µl of 20 mg/ml of protease K. The sample mixture was incubated at 50°C for 18 hours. DNA was extracted by phenol and chloroform followed by ethanol precipitation. DNA was finally dissolved in TE buffer. The small fragments of DNA were removed by 6.5% polyethylene glycol precipitation containing 10 mM $MgCl_2$ twice.

DNA sequencing

Genome sequences of the three strains of zebra-borne EHV-1 (T-616, T-529 and 94-137) were read by the next generation sequencer GS Junior (Roche, USA) according to the manufacturer's protocol. The complete genomes were assembled by reference sequence mapping with Bowtie 2 (33) and editing with Consed (19) and SnapGene (GSL Biotech LLC, USA).

Titration and plaque purification of virus

Virus titers were determined by plaque assay in MDBK cells as described previously (26). In brief, 10-fold dilutions of the viruses were adsorbed onto MDBK cells. After 60 min inoculation at 37°C and 5% CO_2, the inoculum was removed and fresh medium containing 1.5% carboxymethylcellulose was added. After three days incubation at 37°C and 5% CO_2, cells were stained with 0.2% crystal violet solution to determine the plaques counts.

Virus plaque clone and PCR amplification

The methods for plaque purification and condition for PCR amplication were as follows: FEK cell culture in 90 mm dish was inoculated by 10 to 20 viruses per plate, after 1 h incubation, removed virus solution and added MEM containing 1.5% methylcellulose. Two days later, the plaques were picked up and dissolved in MEM. The viruses were propagated in FEK cell for 3 to 4 days. Three μl of virus supernatant was used in PCR mixture for confirmation. Primers used were as follows: Zebra_71-F 5'-ccaacgtaccatcaagtgcggta-3', Zebra_71-R

5'-cgctggtactctcgtaggttgac-3'. PCR was performed by using PrimeSTAR Max Premix (TaKaRa Bio, Japan) with amplification program as follows: the primary hold at 95°C for 4 min, 30 cycles of 98°C 10 sec, 55°C 15 sec, 72°C 45 sec and final extension at 72°C for 2min.

Plaque size measure

For the plaque size measurement, MDBK cells monolayer in 6-well plate were inoculated with viruses for plaque assay. At 3 days inoculation, the cells were fixed and stained by crystal violet solution (0.2% crystal violet, 10% methanol, 10% formalin and 2% sodium acetate). Diameters of approximately 100 randomly selected plaques were measured by using ImageJ software (http://rsbweb.nih.gov/ij/).

Viral growth kinetics

FHK cells in 24-well plate were infected with virus at a MOI of 0.01. After 60 min adsorption, the virus solution was removed, and cells were washed by D-MEM for once time and cultured with fresh D-MEM. Supernatant was collected at 0, 12, 24, 36, 48 and 60 h p.i.. Extracellular titers of each virus sample were determined by plaque assay.

Results

Virus genome structure and Phylogenetic study

The T-616 DNA sequencing indicated to include two viruses, designated T-616 substrains 1 and 2, with lengths of 150,562 bp and 148,847 bp, respectively (GenBank accession nos. KF644573 and KF644574, respectively). The lengths of the T-529 and 94-137 genomes were 147,963 bp and 149,457 bp, respectively (GenBank accession nos. KF644580 and KF644575, respectively). Multiple alignment was examined by MAFTT (28). T529, T616 and 94-137 viral genomes shared 99% identities with each other and shared 98% and 95% identities with the horse derived EHV-1 and EHV-9. Phylogenic analyses based on the whole genome sequences indicated that T-529 and 94-137 are closely related to each other and distantly related to T-616 substrain 1(Fig. 12).

Single nucleotide polymorphisms and insertions and deletions of nucleotides were detected in Consed with whole genome sequence comparison. The differences among the genome lengths are caused by large deletions, variation of tandem repeat sequences including repeats in ORF24 (a homologue of HSV-1 UL36) and ORF71 (a homologue of HSV-1 US5), ORF64 (a homologue of HSV-1 ICP4 gene) downstream and an intergenic region between ORF62 (a homologue of HSV-1 UL1) and ORF63 (a homologue of HSV-1 ICP0 gene).

Two large deletions were observed in T-616 substrain 2 and T-529. A 1,714 bps deletion was found in T-616 substrain 2, corresponding to nucleotides 128,715 to 130,428 in T-616 substrain 1 (Fig. 13A). This deletion caused amino acid sequence mutation with truncation of ORF70 and the lack of ORF71 in T-616 substrain 2 (Fig. 13 A and B). The two substrains of T-616 were cloned by plaque purification and the difference was confirmed by PCR (Fig. 13C). Multi-step virus growth never show the significant difference between T-616

two substrains (Fig. 14A). Also there is not significant difference in plaques size formed by T-616 two substrains (Fig. 14B). On the other hand, the genome of T-529 lacks 1,611 bp region that contains ORF1 and ORF2. Therefore T-529 does not possess proteins encoded by ORF1 and ORF2.

Comparison of ORFs between T-592, T-616, 94-137 and Ab4p strains

The protein sequence variations were identified by BSR (the homology bit score ratio), which was obtained by the blast tool (62). The homology of each protein of EHV-1 against each other strains was calculated as the bit score (BS). BSR was the ratio between the average BS of each strain against Ab4p and the BS of Ab4p against Ab4p. The BSR is lower than 1 if there were variations between Ab4p and the other strains, if there were no difference, the BSR is 1.

pORF68 and pORF71 were found to contain a relatively large amount of variations (BSR<0.85) (Table 2). The gene ORF68 of Ab4p is 1257 bp in length, but that of T-616, 94-137 and T-529 are 945 bp, 942 bp and 942 bp, respectively. This difference was caused by one base deletion of the sequence. The lengths of gene ORF71 in these four viruses are 2394bp, 2625bp, 2520bp, and 2535bp, respectively (Table 2). Even 53 of 75 (70.6%) protein BSRs were higher than 0.98, only protein ORF10 BSR reaches 1 (Table 2). The envelope proteins of virus isolated from onager, zebra and gazelle showed higher conservation than the other essential genes including ORF30 (DNA polymerase) and ORF64 (transcriptional regulator) (Tables 3). Except 94-137 lost a small fragment of 5 amino acid in pORF71, all other envelope proteins are 100% conserved between the T-592, and 94-137 (data not show).

Zebra-borne EHV-1 isolated from Jerka, a polar bear

Greenwood et al. (22) reported nucleotide sequences of ORF10 (a homologue of HSV-1 UL49.5), ORF15 (a homologue of HSV-1 UL45), ORF16 (a homologue of HSV-1 UL44), ORF30, ORF33 (a homologue of HSV-1 UL27) and ORF67 (also called IR6) of the zebra borne EHV-1 isolated from Jerka. The corresponding amino acid sequences of ORF10, ORF30 and ORF67 in the present three zebra-borne EHV-1s are identical to those of the zebra-borne EHV-1 isolated from Jerka(22), although one to four base differences were found among them (Table 4). Amino acid sequence differences were found one in ORF15, two in ORF16 and one in ORF33 between the zebra-borne EHV-1 isoalted from Jerka and the present three zebra-borne EHV-1s. Phylogenic tree prepared by SplitsTree based on a fragment of ORF30 nucleotide sequences is shown in Fig. 15. These data indicated that the zebra borne-EHV-1 isolated from Jerka should be regarded as an almost identical virus to the present three zebra-borne

Discussion

T-529 and 94-137, which are phylogenetically related, were isolated from zoo animals (an onager and a gazelle, respectively) that were kept close to plains zebras (*E. q. burchelli*), while T-616 was isolated from a Grevy's zebra (*E. grevyi*). The phylogenic relatedness among these zebra-borne viruses seems to reflect the phylogenetic relatedness among the host zebra species (8). Two substrains were found in T-616 virus. Although DNA fingerprints were shown in

the report by Wolff et al. (64), it is unclear that the original isolate from the T-616 consisted of two substrains or not.

Cross-species transmission sometime cause fatal disease and the genetic recombination also can induce new pathogen break out. Greenwood et al. (22) discussed that ORF30 of the virus isolated from Jerka was a recombinant gene between those of EHV-1 and EHV-9, with the 5'-portion of the amplicon being EHV1-like, the middle being EHV9-like, and the last 110 bp again being EHV1-like based on computer analysis of amplicon. Although the recombination possibility of this area was evaluated using the same data set in the reference 22, there was not any evidences of recombination in this area, where they insisted that the recombination occurred, by using two programs of SplitsTree (24) and TOPALi (35). If the recombination was scientifically supported, the recombination should be detected using any algorithms for finding recombination. Therefore it is unable to conclude that the zebra-borne EHV-1 isolated from Jerka was a recombinant virus. The three zebra-borne EHV-1 viruses analyzed in the present study and the virus isolated from Jerka might be a subtype of EHV-1 that was derived from the same ancestor virus of EHV-1 (Fig.15). The three viruses investigated this time never show any genetic recombination, in contrast, the virus genomes are kept well except some genes deletion.

Nugent et al. (39) indicated the EHV-1 causing equine herpesvirus myeloencephalopathy should have the neuropathogenic marker of D752 in ORF30. The present three zebra-borne EHV-1 strains have the neuropathogenic marker D752 in ORF30, Other researchers reported that the present three

zebra-borne EHV-1s showed higher pathogenicity than horse strains in hamster, caused severe neurological disease (25).

In recent years, fatal encephalitis induced by the zebra borne equine herpesvirus has been reported frequently (1, 22). The risk of zebra-borne EHV-1 infection in the zoos cannot be ignored.

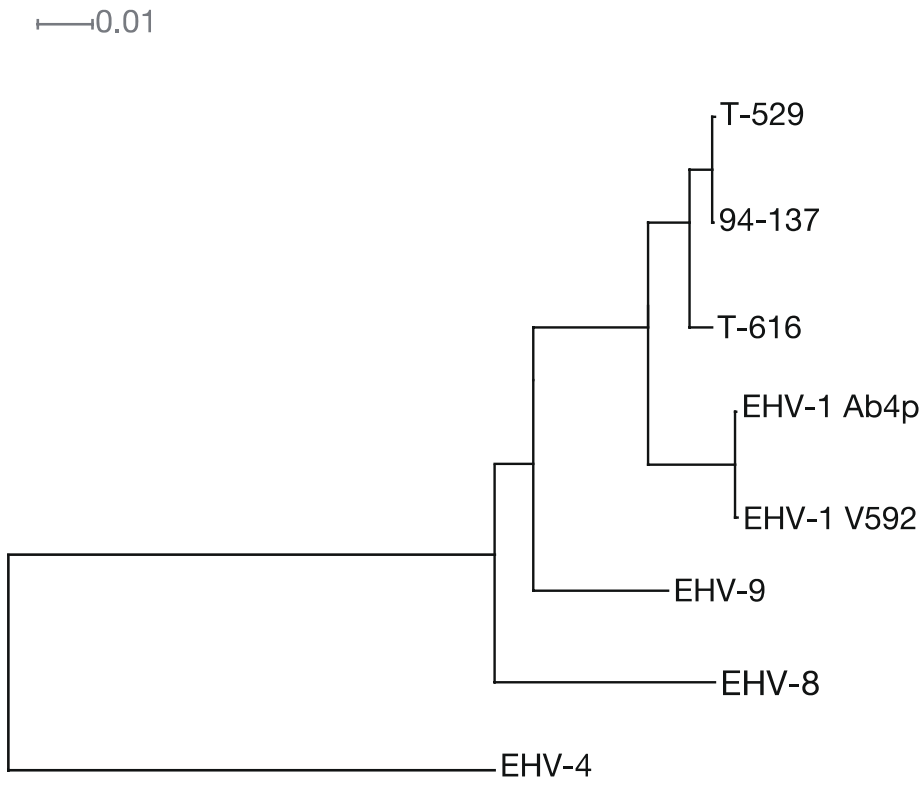

Figure. 12. Neighbor-joining phylogenic tree based on the genome sequences of three zebra-borne EHV-1 (T-616: KF644573; T-529: KF644580; 94-137: KF644575), two horse strains of EHV-1 (Ab4p:AY665713; V592:AY464052), EHV-8 (JQ343919), EHV-9 (AP010838) and EHV-4 (AF030027). All node has 100% bootstrap value. The tree was constructed by SplitsTree. The scale bar is given by average number of mutations per site.

A

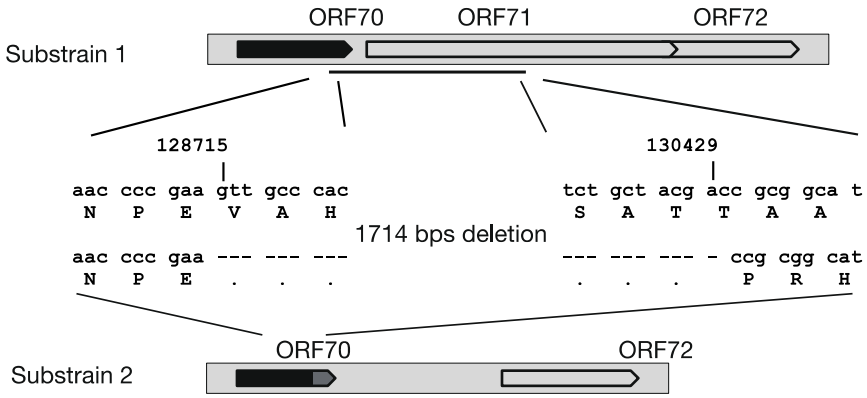

B

Substrain 1 NPEVAHLRSGHSDDSTHTGGASNGIQDCDSQLKTVYACLALIGLGTCAMIGLIVYICVLRSKLSSRDFSRAQNVKHRNYQRLEYVA*

Substrain 2 NPE*PRHSQPSLTHRRSRLRGLHPQPNPAQRLLQKQLLLLPPPRIRSPSHLLQQSLTRPTLPPCPRL**

C

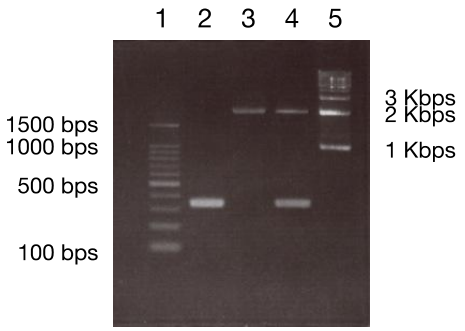

Figure. 13. (A) Nucleotide deletion from the tail part of ORF70 to the head part of ORF71. The arrow in black indicates the original ORF70. The other arrow in dark grey indicates the truncated tail part of ORF70 caused by deletion. (B) Amino acid sequence alignments of the tail part of ORF70 in Substrains 1 and 2. The amino acid sequences with underline indicate the corresponding sequences shown in the panel A. The amino acid sequence in italic grey indicates the truncated tail of ORF70 caused by the deletion. (C) PCR results to confirm the presence of two viruses in T-616. PCR primers used were as follows: Zebra_71-F 5'-ccaacgtaccatcaagtgcggta-3', Zebra_71-R 5'-cgctggtactctcgtaggttgac-3'. PCR was examined by using PrimeSTAR Max Premix (TaKaRa Bio, Japan) with amplification program as follows: the primary hold at 95°C for 4 min, 30 cycles of 98°C 10 sec, 55°C 15 sec, 72°C 45 sec. Lanes were 100 bp ladder marker (1), T-616 substrain 2 (2), T-616 substrain 1 (3), the original seed stock of T-616 (4), 1 kbp ladder marker (5). Expected sizes are 344 bps for T-616 substrain 2 and 2058 bps for T-616 substrain 1.

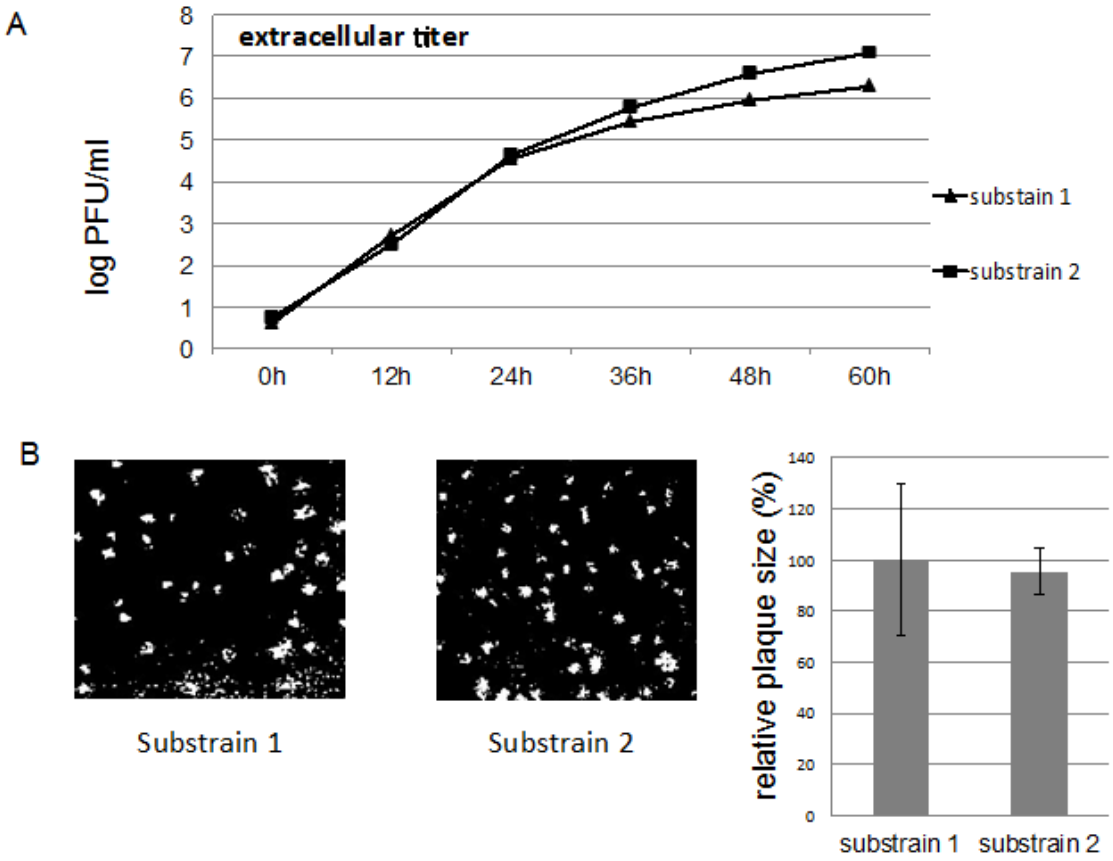

Figure. 14. Growth kinetic and relative plaque size of T-616 two substrains. (A) Multi-step growth of T-616 two substrains in FHK cells. Cell culture solution was harvested at 0, 12, 24, 36, 48, 60 h post inoculation and determined by the titration in MDBK cells. (B) plaque size analysis of T-616 two substrains in MDBK cells.

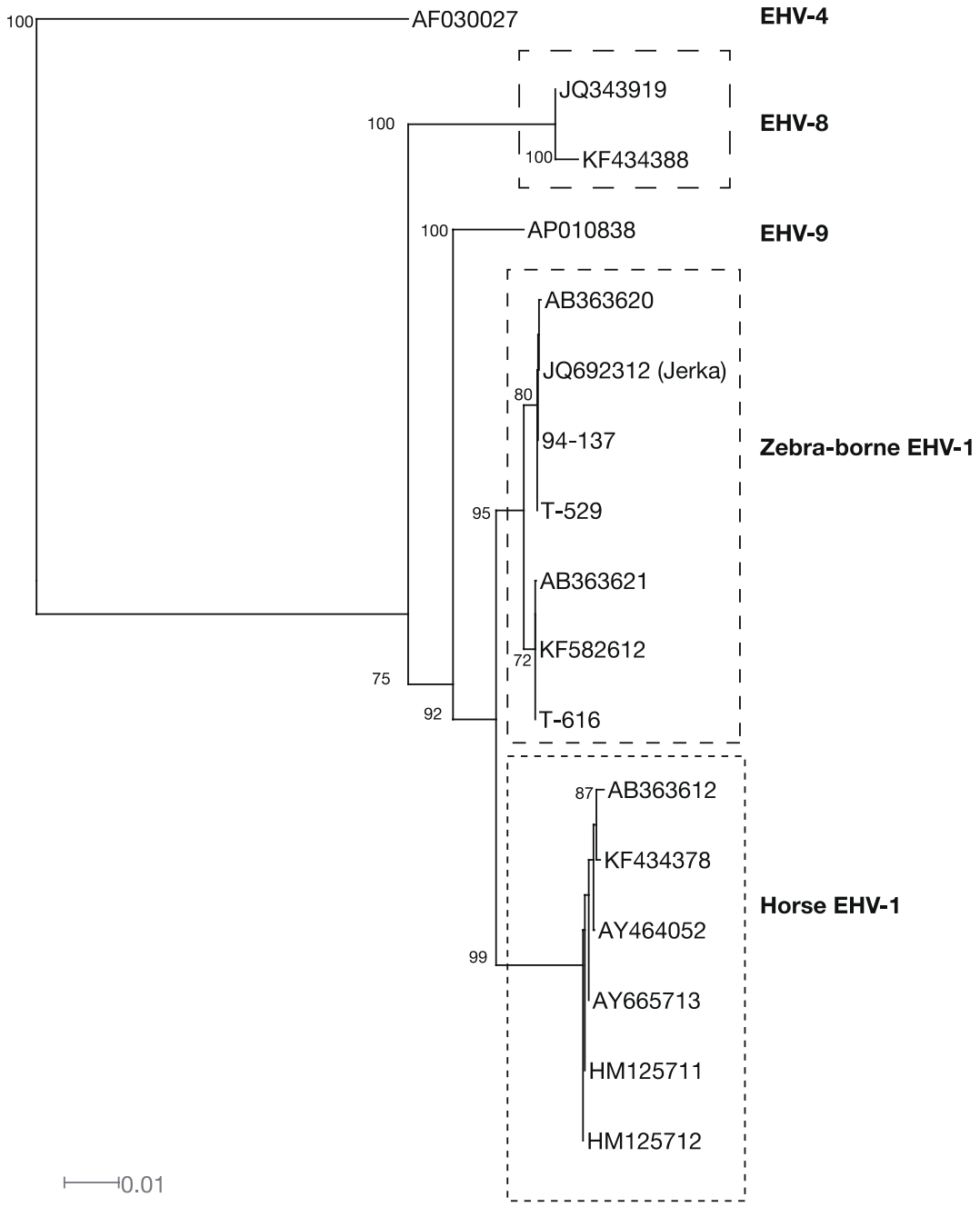

Figure.15. Neighbor-joining phylogenic tree based on nucleotide sequences corresponding to 2023 to 2484 of ORF30. Labels in the tree are accession numbers. All sequences were obtained from GenBank. Numbers are bootstrap values greater than 70%. The tree was constructed by SplitsTree. The scale bar is given by average number of mutations per site.

Table 2. Sequence features and ORFs variations

	EHV-1 Ab4p	T-616	94-137	T-529	BSR
genome length	150224	150561	149457	147757	
G+Ccontents	56.66	56.66	56.60	56.60	
gene	DNA sequence length				
1	609	621	621	0	0.963
2	618	618	618	0	0.975
3	774	774	774	774	0.970
4	603	603	603	603	0.988
5	1413	1413	1413	1413	0.976
6	1032	1032	1032	1032	0.996
7	3246	3240	3246	3246	0.978
8	738	738	738	738	0.990
9	981	981	981	981	0.975
10	303	303	303	303	1.000
11	915	915	915	915	0.975
12	1350	1350	1350	1350	0.986
13	2616	2607	2607	2607	0.967
14	2244	2253	2253	2253	0.983
15	684	660	660	660	0.911
16	1407	1407	1407	1407	0.985
17	1206	1206	1206	1206	0.996
18	1218	1218	1218	1218	0.989

19	1494	1494	1494	1494	0.986
20	966	966	966	966	0.997
21	2373	2373	2373	2373	0.992
22	1398	1398	1398	1398	0.991
23	3063	3063	3063	3063	0.998
24	10266	10392	10320	10398	0.940
25	360	360	360	360	0.997
26	828	828	828	828	0.989
27	423	489	489	489	0.990
28	1863	1863	1863	1863	0.999
29	981	981	981	981	0.997
30	3663	3663	3663	3663	0.984
31	3630	3630	3630	3630	0.997
32	2328	2328	2328	2328	0.995
33	2943	2943	2943	2943	0.999
34	483	483	483	483	0.986
35	1941	1941	1941	1941	0.996
35.5	990	990	990	990	0.995
36	1764	1764	1764	1764	0.994
37	819	819	819	819	0.966
38	1059	1059	1059	1059	0.993
39	2547	2547	2547	2547	0.992
40	1593	1593	1593	1593	0.988
41	720	720	720	720	0.993
42	4131	4131	4131	4131	0.999

43	945	945	945	945	0.999
44 (47)	1173	1173	1173	1173	0.997
45	2121	2121	2121	2121	0.989
46	1113	1110	1110	1110	0.984
48	954	954	954	954	0.969
49	1785	1785	1785	1785	0.991
50	1698	1698	1698	1698	0.994
51	225	225	225	225	0.989
52	1353	1353	1353	1353	0.995
53	2664	2664	2664	2664	0.995
54	2256	2151	2151	2151	0.936
55	912	912	912	912	0.993
56	2262	2262	2262	2262	0.994
57	2646	2646	2646	2646	0.995
58	678	678	678	678	0.998
59	540	540	540	540	0.976
60	639	639	639	639	0.986
61	939	939	939	939	0.969
62	558	657	657	657	0.996
63	1599	1596	1596	1596	0.950
64	4464	4461	4434	4446	0.949
65	882	825	870	825	0.934
66	711	711	711	711	0.950
67	819	825	825	825	0.987
68	1257	945	942	942	0.773

69	1149	1152	1152	1152	0.991
70	1236	1236	1236	1236	0.987
71	2394	2625	2520	2535	0.657
72	1209	1359	1359	1359	0.995
73	1275	1278	1278	1278	0.954
74	1653	1653	1653	1653	0.988
75	393	393	393	393	0.992
76	660	660	660	660	0.956

Each BS mean of zebra, gazelle and onager viruses was divided by the BS of EHV-1. The BS was generated by blast search against EHV-1 protein sequence using each relevant sequence of zebra, gazelle, onager virus and EHV-1 itself. The proteins of ORF1 and ORF2 were not available from onager virus.

Table 3. Genetic identities of ORF30, ORF64 and ORF72 among EHV-1(Ab4p), T-616, 94-137 and T-529

	EHV-1	T-616	94-137	T-529
ORF30 (DNA polymerase)				
EHV-1(Ab4p)		0.984	0.985	0.985
T-616	0.969		0.997	0.997
94-137	0.969	0.993		1.000
T-529	0.970	0.994	0.999	
ORF64 (transcriptional regulator)				
EHV-1(Ab4p)		0.969	0.954	0.956
T-616	0.957		0.981	0.983
94-137	0.938	0.972		0.997
T-529	0.940	0.974	0.997	
ORF72 (glycoprotein D)				
EHV-1(Ab4p)		0.987	0.986	0.986
T-616	0.981		0.999	0.999
94-137	0.980	0.999		1.000
T-529	0.980	0.999	1.000	

Upper right of diagonal square is amino acid sequence identity, and lower left of diagonal space is nucleotide identity.

Table 4. Amino acid differences and synonymous differences among zebra borne EHV-1

Gene	ORF10	ORF15		ORF16			ORF30				ORF33	ORF67	
Covered position	complete gene	1 to 218		complete gene			675 to 954				500 to 878	85 to 198	
Amino acid position	19	216	217	107	150	450	739	754	873	939	516	89	109
T-529	*L(TTG)*	P(CCG)	F(TTT)	E(GAG)	R(CGA)	A(GCC)	L(CTT)	S(TCG)	F(TTC)	K(AAA)	N(AAT)	A(GCA)	V(GTT)
94-137	L(CTG)	P(CCG)	F(TTT)	E(GAG)	R(CGA)	A(GCC)	L(CTT)	S(TCG)	F(TTC)	K(AAA)	N(AAT)	A(GCA)	V(GTT)
T-616	L(CTG)	P(CCG)	F(TTT)	E(GAG)	R(CGA)	*A(GCA)*	*L(CTC)*	*S(TCA)*	*F(TTT)*	*K(AAG)*	N(AAT)	A(GCA)	*V(GTC)*
Polar Bear Jerka	L(CTG)	*P(CCA)*	*I(ATT)*	*Q(CAG)*	*L(CTA)*	A(GCC)	L(CTC)	S(TCG)	*F(TTT)*	K(AAA)	*D(GAT)*	*A(GCC)*	V(GTT)

Differences among the sequences are indicated by italic. Amino acid and codon are shown.

Accession numbers of sequence data of the polar bear Jerka are JQ692315 for ORF10, JQ692311 for ORF15, JQ692313 for ORF16, JQ692312 for ORF30, JQ692316 for ORF33, and JQ692314 for ORF67.

GENERAL CONCLUSIONS

EHV-9 was isolated from a Thomson's gazelle suffering neurological disease in Japan, and is most closely to neurological EHV-1 (16). EHV-9 inducing deaths of encephalitis in various animals have been reported all over the world (7, 11, 27). Elucidation of the neuropathogenesis of EHV-9 is very important, and it also contributes to analysis of neuropathogenesis of EHV-1. However, EHV-9 pathogenesis is pooly understood.EHV-1 is a major pathogen in horses and causes abortion, respiratory infection, and neurological disorders (4, 55). In recent years, equine herpesviruses have been isolated from non-equine species including gazelle, giraffe, and polar bears (18, 22, 27). The cross-species infection may induce severe disease in non-host species.

The main objective of this study was to investigate the attenuated mutant EHV-9 viruses to identify the gene associated with the attenuation. And, the author also studied the phylogenic relatedness of three zebra-borne EHV-1s to evaluate the possibility of genetic recombination of EHV-1 and EHV-9.

In chapter 1, the alteration of non-stop ORF19 mRNA of SP21 was investigated. SP21 is a mutant of EHV-9 and showed low virulence in hamster. SP21 full-genome was analyzed and two point mutants in ORF14 and ORF19 have been identified. The point mutant in ORF19 causes mutation from a stop codon to a sense codon. The non-stop mRNA in mammalian cells is degraded fast by non-stop decay. On the other hand, some researcher found no degradation of the non-stop mRNA. The studies of non-stop ORF19 mRNA of SP21 showed the non-stop mRNA had the same poly-A tail to the wild type ORF19 mRNA. There was no significant difference on the quantity of both of the non-stop and

wild type ORF19 mRNAs. pORF19 could be detected in the EHV-9 infected cells. On the other hand, the non-stop pORF19 of SP21 was not detected. It was suggested that the non-stop pORF19 in infected cells was smaller in amount than the wild type pORF19. It was unclear that the expression of the non-stop protein was repressed or degraded by proteasome.

In chapter 2, the author repaired the mutations in ORF14 or ORF19 in SP21, named SP21-14R and SP21-19R. EHV-9, SP21, SP21-14R and SP21-19R were investigated their virulence, and confirmed the mutation related to the virulence *in vitro* and *in vivo*. SP21-14R formed the larger plaques than wild type EHV-9, although the plaques formed by SP21 is similar to EHV-9. On the other hand, SP21-19R formed the plaques smaller than those of other three viruses. It was suggested that pORF14 enhances virus expansion, and pORF19 down-regulate this activity. The multi-step virus growth experiment showed that SP21 and SP21-14R replicated similar to the wild type EHV-9, and SP21-19R extracellular titer was approximately 50-fold lower than that of the wild type EHV-9. The mutation of pORF19 did not affect the virus growth in culture cells. The pathogenicity analysis of these four viruses by using hamster showed that EHV-9 and SP21-19R caused neurological symptoms and died. On the other hand, hamster inoculated with SP21 and SP21-14R recovered after a short period of neurological disorders. The results suggested that pORF19 might be related to the pathogenicities of EHV-9.

In chapter 3, the full genome sequences of three zebra-borne EHV-1s isolated from onager, zebra and gazelle (T-529, T-616 and 94-137, respectively) were determined. The genome structure and phylogenic study showed three viruses are close to horse EHV-1. Phylogenic analyses based on the whole

genome sequences indicated that T-529 and 94-137 are closely related to each other and distantly related to T-616. Zoo animals from which T-529 or 94-137 was isolated were kept close to plains zebras, and T-616 was isolated from Grevy's zebra. The phylogenic relatedness among these zebra-borne viruses seems to reflect the phylogenetic relatedness among the host zebra species (8). The comparison of ORFs between T-592, T-616, 94-137 and Ab4p strains suggested that genes encode envelope proteins are high conservation. Greenwood et al. (22) reported an equine herpesvirus infected to a polar bear in Berlin was a EHV-1 and EHV-9 recombinant virus. However, the present data indicated that the zebra borne-EHV-1 isolated from Jerka should be regarded as an almost identical virus to the present three zebra-borne EHV-1s.

The main finding of this study can be summarized in the following points.

1. Non-stop gene ORF19 of EHV-9 mutant strain SP21 never show any difference by comparing with the wild-type EHV-9 on mRNA level. The expression of non-stop gene ORF19 of SP21 is lower than that of wild type in infected cells. The amount of non-stop pORF19 in SP21 virion is about 20% of wild type EHV-9 and increases after ORF14 mutantation repaired.
2. The mutantation of ORF14 related to the virus growth in cell culture, on the other hand, that gene ORF19 did not affect virus replication *in vitro*. Gene ORF14 enhances the virus expansion, and gene ORF19 down regulates the virus spread. EHV-9 mutant strain SP21 and ORF14 repaired SP21-14R showed low virulence in hamster infection model, in contrast, ORF19 repaired SP21-19R showed high virulence in hamster like wild type EHV-9. It suggested that mutation of ORF19 related to the pathogenicity attenuation.

3. The phylogenic relatedness among zebra-borne EHV-1s, T-529, T-616 and 94-137 isolated from onager, zebra and gazelle, respectively, reflected the phylogenic relatedness among the host zebra species. T-529 and 94-137 isolated from onager and gazelle which kept near plains zebras showed close relatedness, and T-616 was isolated from Grevy's zebra. The Protein variant studies showed that EHV-1 was different from HSV-1 in genes reservation (data not show).
4. The virus isolated from polar bear in Berlin was not a EHV-1 and EHV-9 recombinant virus. The zebra-borne EHV-1s investigated never showed any genetic recombination, in contrast, virus genomes were well conserved, specially the genes encoding glycoproteins.

The findings of this study provide a phenomenon observation of a virus gene without stop codon in mammalian cells. The findings explain a gene related to the pathogenicity of EHV-9. The studies of 3 zebra-borne EHV-1s may provide a important information about a EHV-1 infection occurred on zoo animals.

ACKNOWLEDGMENTS

First I would like to express my heartfelt gratitude and indebtedness to my professor Dr. Hideto Fukushi, Laboratory of Veterinary Microbiology, Department of Applied Veterinary Science, Faculty of Applied Biological Sciences, Gifu University, for accepting me to study here, for his support, encouragement, kind direction and critical review throughout the experiments and in the preparation of this thesis.

I am thankful to Associate Professor Dr. Kenji Ohya, Department of Applied Veterinary Science, Faculty of Applied Biological Sciences, Gifu University, for his support, valuable suggestions and technical advice.

I also greatly indebted to Professor Dr. Naotaka Ishiguro, Laboratory of Food and Environmental Hygiene, Faculty of Applied Biological Science, Gifu University; Professor Dr. Tetsuya Mizutani, Research and Education Center for Prevention of Global Infectious Disease of Animals, Faculty of Agriculture, Tokyo University of Agriculture and Technology; Professor Dr. Kenji Murakami, Laboratory of Veterinary Microbiology, Faculty of Agriculture; Professor Dr. Haruko Ogawa, Diagnostic Center for Animal Hygiene and Food Safety, Obihiro University of Agriculture and Veterinary Medicine for their valuable comments, criticisms and patiently revising this thesis.

I want to thank graduate students and all members in the laboratory of Veterinary Microbiology for their cooperation, assistance and help in many ways. And I also want to thank Professor Dr. Tokuma Yanai, Laboratory of Veterinary Pathology, Gifu University and the members in the laboratory of veterinary pathology for encouragement and technical support.

I also want to thank all animals used in my experiments.

I wish to express my deeply gratitude to my ex-professor Abe Jun for his encouragement and support to my dream. I never forget your kindness and help.

I would like to thank my friend Amira Ahmed Hassan Abdelaziz for her encouragement and helpful advises to my experiments, for her kindly support to my life in Japan.

At last, I thank my loving father for his endless support and love that make me strive for the dream.

REFERENCES

1) Abdelgawad, A., Azab, W., Damiani, A. M., Baumgartner, K., Will, H., Osterrieder, N., and Greenwood, A. D. (2014). Zebra-borne equine herpesvirus type 1 (EHV-1) infection in non-African captive mammals. Vet. Microbiol. 169, 102~106.

2) Akimitsu, N., Tanaka, J., and Pelletier, J. (2007). Translation of nonSTOP mRNA is repressed post-initiation in mammalian cells. EMBO. J 26, 2327~2338.

3) Allen, G. P., Yeargan, M. R., and Bryans, J. T. (1983). Alterations in the equine herpesvirus 1 genome after in vitro and in vivo virus passage. Infect. Immun. 40, 436~439.

4) Allen, G. P., Yeargan, M. R., Turtinen, L. W., and Bryans, J. T. (1985). A new field strain of equine abortion virus (equine herpesvirus-1) among Kentucky horses. Am. J. Vet. Res. 46, 138~140.

5) Bengtson, M. H., and Joazeiro, C. A. (2010). Role of a ribosome-associated E3 ubiquitin ligase in protein quality control. Nature 467, 470~473.

6) Blunden, A. S., Smith, K. C., Whitwell, K. E., and Dunn, K. A. (1998). Systemic infection by equid herpesvirus-1 in a Grevy's zebra stallion (Equus grevyi) with particular reference to genital pathology. J. Comp. Pathol. 119, 485~493.

7) Borchers, K., Lieckfeldt, D., Ludwig, A., Fukushi, H., Allen, G., Fyumagwa, R., and Hoare, R. (2008). Detection of Equid herpesvirus 9 DNA

in the trigeminal ganglia of a Burchell's zebra from the Serengeti ecosystem. J. Vet. Med. Sci. 70, 1377~1381.

8) Cote, O., Viel, L., and Bienzle, D. (2013). Phylogenetic relationships among Perissodactyla: secretoglobin 1A1 gene duplication and triplication in the Equidae family. Mol. Phylogenet. Evol. 69, 430~436.

9) Dauber, B., Pelletier, J., and Smiley, J. R. (2011). The herpes simplex virus 1 vhs protein enhances translation of viral true late mRNAs and virus production in a cell type-dependent manner. J. Virol. 85, 5363~5373.

10) Doma, M. K., and Parker, R. (2006). Endonucleolytic cleavage of eukaryotic mRNAs with stalls in translation elongation. Nature 440, 561~564.

11) Donovan, T. A., Schrenzel, M. D., Tucker, T., Pessier, A. P., Bicknese, B., Busch, M. D., Wise, A. G., Maes, R., Kiupel, M., McKnight, C., and Nordhausen, R. W. (2009). Meningoencephalitis in a polar bear caused by equine herpesvirus 9 (EHV-9). Vet. Pathol. 46, 1138~1143.

12) El~Habashi, N., El~Nahass el, S., Fukushi, H., Hibi, D., Sakai, H., Sasseville, V., and Yanai, T. (2010). Experimental intranasal infection of equine herpesvirus 9 (EHV-9) in suckling hamsters: kinetics of viral transmission and inflammation in the nasal cavity and brain. J. Neurovirol. 16, 242~248.

13) Esclatine, A., Taddeo, B., and Roizman, B. (2004). The UL41 protein of herpes simplex virus mediates selective stabilization or degradation of cellular mRNAs. Proc. Natl. Acad. Sci. U S A 101, 18165~18170.

14) Feng, X., Thompson, Y. G., Lewis, J. B., and Caughman, G. B. (1996). Expression and function of the equine herpesvirus 1 virion-associated host

shutoff homolog. J. Virol. 70, 8710~8718.

15) Fukushi, H., Taniguchi, A., Yasuda, K., Yanai, T., Masegi, T., Yamaguchi, T., and Hirai, K. (2000). A hamster model of equine herpesvirus 9 induced encephalitis. J. Neurovirol. 6, 314~319.

16) Fukushi, H., Tomita, T., Taniguchi, A., Ochiai, Y., Kirisawa, R., Matsumura, T., Yanai, T., Masegi, T., Yamaguchi, T., and Hirai, K. (1997). Gazelle herpesvirus 1: a new neurotropic herpesvirus immunologically related to equine herpesvirus 1. Virology 227, 34~44.

17) Fukushi, H., Yamaguchi, T., and Yamada, S. (2012). Complete genome sequence of equine herpesvirus type 9. J. Virol. 86, 13822.

18) Ghanem, Y. M., Fukushi, H., Ibrahim, E. S., Ohya, K., Yamaguchi, T., and Kennedy, M. (2008). Molecular phylogeny of equine herpesvirus 1 isolates from onager, zebra and Thomson's gazelle. Arch. Virol. 153, 2297~2302.

19) Gordon, D., and Green, P. (2013). Consed: a graphical editor for next-generation sequencing. Bioinformatics 29, 2936~2937.

20) Gray, W. L., Baumann, R. P., Robertson, A. T., Caughman, G. B., O'Callaghan, D. J., and Staczek, J. (1987a). Regulation of equine herpesvirus type 1 gene expression: characterization of immediate early, early, and late transcription. Virology 158, 79~87.

21) Gray, W. L., Baumann, R. P., Robertson, A. T., O'Callaghan, D. J., and Staczek, J. (1987b). Characterization and mapping of equine herpesvirus type 1 immediate early, early, and late transcripts. Virus. Res. 8, 233~244.

22) Greenwood, A. D., Tsangaras, K., Ho, S. Y., Szentiks, C. A., Nikolin, V. M., Ma, G., Damiani, A., East, M. L., Lawrenz, A., Hofer, H., and Osterrieder, N. (2012). A potentially fatal mix of herpes in zoos. Curr. Biol.

22, 1727~1731.

23) Hubert, P. H., Birkenmaier, S., Rziha, H. J., and Osterrieder, N. (1996). Alterations in the equine herpesvirus type-1 (EHV-1) strain RacH during attenuation. Zentralbl Veterinarmed B 43, 1~14.

24) Huson, D. H., and Bryant, D. (2006). Application of phylogenetic networks in evolutionary studies. Mol. Biol. Evol. 23, 254~267.

25) Ibrahim, E. S., Kinoh, M., Matsumura, T., Kennedy, M., Allen, G. P., Yamaguchi, T., and Fukushi, H. (2007). Genetic relatedness and pathogenicity of equine herpesvirus 1 isolated from onager, zebra and gazelle. Arch. Virol. 152, 245~255.

26) Ibrahim, E. S. M., Pagmajav, O., Yamaguchi, T., Matsumura, T., and Fukushi, H. (2004). Growth and virulence alterations of equine herpesvirus 1 by insertion of a green fluorescent protein gene in the intergenic region between ORFs 62 and 63. Microbiol. and Immunol. 48, 831~842.

27) Kasem, S., Yamada, S., Kiupel, M., Woodruff, M., Ohya, K., and Fukushi, H. (2008). Equine herpesvirus type 9 in giraffe with encephalitis. Emerg. Infect. Dis. 14, 1948~1849.

28) Katoh, K., and Standley, D. M. (2013). MAFFT multiple sequence alignment software version 7: improvements in performance and usability. Mol. Biol. Evol. 30, 772~780.

29) Kennedy, M. A., Ramsay, E., Diderrich, V., Richman, L., Allen, G. P., and Potgieter, L. N. D. (1996). Encephalitis associated with a variant of equine herpesvirus 1 in a Thomson's gazelle (Gazella thomsoni). Journal of Zoo and Wildlife Medicine 27, 533~538.

30) Klauer, A. A., and van Hoof, A. (2012). Degradation of mRNAs that lack

a stop codon: a decade of nonstop progress. Wiley. Interdiscip. Rev. RNA 3, 649~660.

31) Kodama, A., Yanai, T., Yomemaru, K., Sakai, H., Masegi, T., Yamada, S., Fukushi, H., Kuraishi, T., Hattori, S., and Kai, C. (2007). Acute neuropathogenicity with experimental infection of equine herpesvirus 9 in common marmosets (Callithrix jacchus). J. Med. Primatol. 36, 335~342.

32) Kritas, S. K., Pensaert, M. B., and Mettenleiter, T. C. (1994). Role of envelope glycoproteins gI, gp63 and gIII in the invasion and spread of Aujeszky's disease virus in the olfactory nervous pathway of the pig. J. Gen. Virol. 75 (Pt 9), 2319~2327.

33) Langmead, B., and Salzberg, S. L. (2012). Fast gapped-read alignment with Bowtie 2. Nat. Methods. 9, 357~359.

34) Mardis, E. R. (2008). Next-generation DNA sequencing methods. Annual Review of Genomics and Human Genetics 9, 387~402.

35) Milne, I., Wright, F., Rowe, G., Marshall, D. F., Husmeier, D., and McGuire, G. (2004). TOPALi: software for automatic identification of recombinant sequences within DNA multiple alignments. Bioinformatics 20, 1806~1807.

36) Montali, R. J., Allen, G. P., Bryans, J. T., Phillips, L. G., and Bush, M. (1985). Equine herpesvirus type 1 abortion in an onager and suspected herpesvirus myelitis in a zebra. J. Am. Vet. Med. Assoc. 187, 1248~1249.

37) Mukhopadhyay, A., Lee, G. E., and Wilson, D. W. (2006). The amino terminus of the herpes simplex virus 1 protein Vhs mediates membrane association and tegument incorporation. J. Virol. 80, 10117~10127.

38) Narita, M., Uchimura, A., Kimura, K., Tanimura, N., Yanai, T., Masegi, T.,

Fukushi, H., and Hirai, K. (2000). Brain lesions and transmission of experimental equine herpesvirus type 9 in pigs. Vet. Pathol. 37, 476~479.

39) Nugent, J., Birch-Machin, I., Smith, K. C., Mumford, J. A., Swann, Z., Newton, J. R., Bowden, R. J., Allen, G. P., and Davis-Poynter, N. (2006). Analysis of equid herpesvirus 1 strain variation reveals a point mutation of the DNA polymerase strongly associated with neuropathogenic versus nonneuropathogenic disease outbreaks. J. Virol. 80, 4047~4060.

40) Pan, D., and Coen, D. M. (2012). Net -1 frameshifting on a noncanonical sequence in a herpes simplex virus drug-resistant mutant is stimulated by nonstop mRNA. Proc. Natl. Acad. Sci. U. S. A. 109, 14852~14857.

41) Rebhun, W. C., Jenkins, D. H., Riis, R. C., Dill, S. G., Dubovi, E. J., and Torres, A. (1988). An epizootic of blindness and encephalitis associated with a herpesvirus indistinguishable from equine herpesvirus I in a herd of alpacas and llamas. J. Am. Vet. Med. Assoc. 192, 953~956.

42) Saito, S., Hosoda, N., and Hoshino, S. (2013). The Hbs1-Dom34 protein complex functions in non-stop mRNA decay in mammalian cells. J. Biol. Chem. 288, 17832~17843.

43) Sanfilippo, C. M., Chirimuuta, F. N. W., and Blaho, J. A. (2004). Herpes simplex virus type 1 immediate-early gene expression is required for the induction of apoptosis in human epithelial HEp-2 cells. J. Virol. 78, 224~239.

44) Shendure, J., and Ji, H. L. (2008). Next-generation DNA sequencing. Nature Biotechnology 26, 1135~1145.

45) Shu, M., Taddeo, B., Zhang, W., and Roizman, B. (2013). Selective degradation of mRNAs by the HSV host shutoff RNase is regulated by the

UL47 tegument protein. Proc. Natl. Acad. Sci. U. S. A. 110, E1669~1675.

46) Smith, R. H., Caughman, G. B., and Ocallaghan, D. J. (1992). Characterization of the Regulatory Functions of the Equine Herpesvirus-1 Immediate-Early Gene-Product. J. Virol. 66, 936~945.

47) Smith, T. J., Ackland-Berglund, C. E., and Leib, D. A. (2000). Herpes simplex virus virion host shutoff (vhs) activity alters periocular disease in mice. J. Virol. 74, 3598~3604.

48) Strunk, U., Saffran, H. A., Wu, F. W., and Smiley, J. R. (2013). Role of herpes simplex virus VP11/12 tyrosine-based motifs in binding and activation of the Src family kinase Lck and recruitment of p85, Grb2, and Shc. J. Virol. 87, 11276~11286.

49) Studdert, M. J., Fitzpatrick, D. R., Browning, G. F., Cullinane, A. A., and Whalley, J. M. (1986). Equine herpesvirus genomes: heterogeneity of naturally occurring type 4 isolates and of a type 1 isolate after heterologous cell passage. Arch. Virol. 91, 375~381.

50) Sugahara, Y., Matsumura, T., Kono, Y., Honda, E., Kida, H., and Okazaki, K. (1997). Adaptation of equine herpesvirus 1 to unnatural host led to mutation of the gC resulting in increased susceptibility of the virus to heparin. Arch. Virol. 142, 1849~1856.

51) Taddeo, B., Zhang, W., and Roizman, B. (2006). The U(L)41 protein of herpes simplex virus 1 degrades RNA by endonucleolytic cleavage in absence of other cellular or viral proteins. Proc. Natl. Acad. Sci. U. S. A. 103, 2827~2832.

52) Taddeo, B., Zhang, W., and Roizman, B. (2013). The herpes simplex virus host shutoff RNase degrades cellular and viral mRNAs made before infection

but not viral mRNA made after infection. J. Virol. 87, 4516~4522.

53) Taniguchi, A., Fukushi, H., Matsumura, T., Yanai, T., Masegi, T., and Hirai, K. (2000a). Pathogenicity of a new neurotropic equine herpesvirus 9 (gazelle herpesvirus 1) in horses. J. Vet. Med. Sci. 62, 215~218.

54) Taniguchi, A., Fukushi, H., Yanai, T., Masegi, T., Yamaguchi, T., and Hirai, K. (2000b). Equine herpesvirus 9 induced lethal encephalomyelitis in experimentally infected goats. Arch. Virol. 145, 2619~2627.

55) Telford, E. A., Watson, M. S., McBride, K., and Davison, A. J. (1992). The DNA sequence of equine herpesvirus-1. Virology 189, 304~316.

56) Telford, E. A., Watson, M. S., Perry, J., Cullinane, A. A., and Davison, A. J. (1998). The DNA sequence of equine herpesvirus-4. J. Gen. Virol. 79 (Pt 5), 1197~1203.

57) Torres-Torronteras, J., Rodriguez-Palmero, A., Pinos, T., Accarino, A., Andreu, A. L., Pintos-Morell, G., and Marti, R. (2011). A Novel Nonstop Mutation in TYMP does not Induce Nonstop mRNA Decay in a MNGIE Patient with Severe Neuropathy. Human Mutation 32, E2061~E2068.

58) Vittone, V., Diefenbach, E., Triffett, D., Douglas, M. W., Cunningham, A. L., and Diefenbach, R. J. (2005). Determination of interactions between tegument proteins of herpes simplex virus type 1. J. Virol. 79, 9566~9571.

59) Volkening, J. D., and Spatz, S. J. (2009). Purification of DNA from the cell-associated herpesvirus Marek's disease virus for 454 pyrosequencing using micrococcal nuclease digestion and polyethylene glycol precipitation. Journal of Virological Methods 157, 55~61.

60) Wagner, M. J., and Smiley, J. R. (2009). Herpes simplex virus requires VP11/12 to induce phosphorylation of the activation loop tyrosine (Y394) of

the Src family kinase Lck in T lymphocytes. J. Virol. 83, 12452~12461.

61) Wagner, M. J., and Smiley, J. R. (2011). Herpes Simplex Virus Requires VP11/12 To Activate Src Family Kinase-Phosphoinositide 3-Kinase-Akt Signaling. J. Virol. 85, 2803~2812.

62) Watson, G., Xu, W., Reed, A., Babra, B., Putman, T., Wick, E., Wechsler, S. L., Rohrmann, G. F., and Jin, L. (2012). Sequence and comparative analysis of the genome of HSV-1 strain McKrae. Virology 433, 528~537.

63) Weir, J. P. (2001). Regulation of herpes simplex virus gene expression. Gene. 271, 117~130.

64) Wolff, P. L., Meehan, T. P., Basgall, E. J., Allen, G. P., and Sundberg, J. P. (1986). Abortion and perinatal foal mortality associated with equine herpesvirus type 1 in a herd of Grevy's zebra. J. Am. Vet. Med. Assoc. 189, 1185~1186.

65) Yanai, T., Fujishima, N., Fukushi, H., Hirata, A., Sakai, H., and Masegi, T. (2003a). Experimental infection of equine herpesvirus 9 in dogs. Vet. Pathol. 40, 263~267.

66) Yanai, T., Tujioka, S., Sakai, H., Fukushi, H., Hirai, K., and Masegi, T. (2003b). Experimental infection with equine herpesvirus 9 (EHV-9) in cats. J. Comp. Pathol. 128, 113~118.

67) Zhang, Y., Sirko, D. A., and McKnight, J. L. (1991). Role of herpes simplex virus type 1 UL46 and UL47 in alpha TIF-mediated transcriptional induction: characterization of three viral deletion mutants. J. Virol. 65, 829~841.